Control Theory in Biology: From MCA to Chemotaxis

Tau-Mu Yi
tmy@caltech.edu
Division of Biology
Caltech
Pasadena, CA
USA 91125

Pablo Iglesias
pi@jhu.edu
Dept. of Electrical and
Computer Engineering
Johns Hopkins University
Baltimore, MD
USA 21218

Brian Ingalls
bingalls@math.uwaterloo.ca
Dept. of Applied Mathematics
University of Waterloo
Waterloo, Ontario
Canada N2L 3G1

The goal of the tutorial is to introduce Systems Biologists to the application of control theory to biology. The tools of systems and control theory have been instrumental in the successful design of countless man-made complex systems. Biologists, who are trying to reverse engineer complex living networks, can benefit from the insights this theory can provide into the design of biological systems. Of particular importance is understanding the role of feedback control in ensuring the robust behavior of biological processes subjected to internal and external disturbances.

The intended audience is the general Systems Biology community. We will not assume technical knowledge beyond what a typical biologist would be exposed to as an undergraduate and graduate student. Relevant biological examples will be used to give a feel for more abstract concepts, followed up by mathematical explanations that are presented in detail in the handouts. Prerequisites: understanding of chemical and enzyme kinetics, familiarity with ordinary differential equations and linear algebra.

Tutorial Content

The tutorial will begin with a discussion of the connections between control theory and Metabolic Control Analysis (MCA). This section will serve as an introduction to sensitivity analysis and some of the basic tools of control theory. The next section will cover a specific control structure which plays a vital role in man-made and biological mechanisms – integral control. The final section will examine the use of feedback, both positive and negative, in cellular signaling systems. The emphasis will be on building intuition through simple models and then extending this intuition with a more mathematical description. There will be pointers to appropriate references for those who wish to study a topic area in more detail. We hope that the attendees will come away from the tutorial with an appreciation for the importance of feedback structures in biological networks and an appreciation for the contribution which control theory can make in elucidating the behaviour of these systems.

A detailed description of the material to be presented in each section is as follows:

1. A Control Theoretic Approach to Metabolic Control Analysis

The field of Metabolic Control Analysis was developed to address the issues of control and regulation in metabolic networks. Working from a rigorous mathematical foundation, this theory aims to quantify the sensitivity of components of a network to perturbations, as well as to identify the inherent relationships between these sensitivities. This analysis leads to an improved understanding of the nature of the network. Sensitivity analysis also plays a crucial role in the theory of control engineering, as sensitivity and robustness are key issues which must be addressed in any control system design.

We will provide a brief introduction to MCA and to some of the basics of control theory before outlining some of their interconnections. Tools from control theory allow a generalization of the basic

sensitivity analysis of MCA, which deals primarily with steady-state system response to small, constant perturbations. We will examine how the steady state and transient response to small time-varying perturbations can be addressed, and how the theory can be extended beyond the linear regime. Finally, we present an analysis of the main results of MCA – the Summation and Connectivity Theorems – from a control engineer's perspective.

Integral Feedback Control: From Homeostasis to Chemotaxis

In integral feedback control, the output error is integrated and then fed back into the system. This type of control produces robust perfect regulation: the steady-state error approaches zero in the presence of internal and external perturbations. Integral feedback is used ubiquitously in man-made systems, and is likely to be a common control strategy in biological systems. In this section of the tutorial we will cover the following topics:

(a) Examples of integral feedback control in biology from the molecular level (signal transduction) to the organismal level (hormone physiology).

(b) Basic concepts in control theory illustrated by integral feedback. (c) The connection between integral feedback and homeostasis described by the Internal Model Principle.

(d) Implementing a robust differentiator using integral feedback: the preferred chemotactic strategy for motile organisms?

Cellular communication: Uses of positive and negative feedback

Engineering systems use feedback — both positive and negative — to achieve a variety of tasks. Specifically: negative feedback is used to stabilize systems, to reject disturbances, and to improve the robustness of systems. Amplifiers and oscillators rely on the use of positive feedback, as do digital switches. To a large extent, signal transduction pathways are nothing but biological feedback controllers. In this section of the tutorial we will examine mathematically how feedback accomplishes these tasks and illustrate each of them with examples in biological signalling networks.

1 A Control Theoretic Approach to Metabolic Control Analysis

1.1 Introduction

Much work has been devoted to determining the responses of biochemical networks to changes in their environment or their internal components. These studies have been motivated both by direct application to metabolic engineering and pharmaceutics as well as by the desire to improve our understanding of the behaviour of these systems.

This sensitivity analysis has focussed primarily on the steady state (i.e. asymptotic) response of a system to constant (i.e. step) changes in parameters. This is in part due to the relative difficulty of obtaining experimental data on time-varying behaviour as opposed to measurements of steady states. Moreover, in many cases steady state analysis is of primary interest; mechanisms which are under homeostatic control tend to maintain steady-state behaviour with only small and often insignificant transients. In such cases, steady state analysis provides a perfectly adequate description of system behaviour.

However, there are cases in which a dynamic analysis of system response is crucial. This is clearly the case for mechanisms whose nominal behaviour is time-varying, e.g. the cell cycle. Furthermore, even systems for which steady-state behaviour is the norm exhibit dynamic responses to time-varying perturbations, and such nonconstant disturbances are ubiquitous in the cellular environment. Investigation of the transient behaviour invoked in signal transduction networks or the role of Ca^{2+} oscillations as a second messenger demand a dynamic analysis. This paper represents a step towards extending the classical steady state sensitivity analysis to this more general case.

Analytic tools for the study of the sensitivity of biochemical systems have been developed within the fields of Metabolic Control Analysis (MCA) [35, 18, 26] and Biochemical Systems Theory (BST) [58, 67]. This analysis is carried out in a linear (or log-linear) regime in which only small perturbations are addressed. This restriction is necessary since it is only after linearization that the analysis becomes tractable. In particular, the main results of MCA – the Summation and Connectivity Theorems – are only valid in the domain of this local analysis.

The same approach is taken here – the linearized response of a biochemical system is considered. The sensitivity analysis is extended by considering the response not just to constant parameter changes, but also to time varying perturbations. This is achieved through a *frequency domain* analysis which describes the response of the system to a canonical set of inputs (sinusoids). The response to arbitrary perturbations can be reconstructed from this analysis by use of the Fourier transform.

This analysis can be interpreted as an extension of MCA by defining control and response coefficients as functions of the frequency of the oscillatory perturbation. The stoichiometric nature of the network imposes constraints on the system behaviour which can be expressed by generalizations of the Theorems of MCA.

Other generalizations of MCA to time-varying behaviour have appeared in the literature. Analysis of time-varying sensitivity was carried out in [1, 24, 33, 37, 40]. The work presented in [12, 55] is closely related to this paper, as it makes use of Fourier analysis to treat oscillatory behaviour. In those papers the authors investigate the sensitivity of a forced oscillating system to step changes in its parameter values, which is an orthogonal approach to that taken here. In the current work, the system is assumed to be at steady state in the absence of disturbances, and the response to time varying perturbations is examined. A similar analysis has been carried out in [56].

1.2 Linear Model of a Stoichiometric Network

A network consisting of n chemical species involved in m reactions is modelled. The n-vector $\mathbf{s}$ is composed of the concentrations of each species. The constant r-vector $\mathbf{p}$ is composed of the (external) parameters of interest in the model. The m-vector valued function $\mathbf{v} = \mathbf{v}(\mathbf{s}, \mathbf{p})$ describes the rate of each reaction as a function of species concentrations and parameter values. Finally the n by m stoichiometry matrix $\mathbf{N}$ describes the network: component $\mathbf{N}_{i,j}$ is equal to the net number of individuals of species i produced or consumed in reaction j. The network can then be modelled by the ordinary differential equation

$$\frac{d}{dt}\mathbf{s}(t) = \mathbf{N}\mathbf{v}(\mathbf{s}(t), \mathbf{p}) \qquad \text{for all } \ t \geq 0. \tag{1}$$

The vector $\mathbf{p}$ contains any external parameters which have a direct effect on the rates of the reactions (e.g. kinetic constants of enzymes and external effectors).

Before embarking on an analysis of system (1) it is prudent to first consider any linear dependencies inherent in the state variables of the system (which will simplify both the analysis and the computation). Each structural conservation (e.g. conserved moiety) in the network corresponds to a linearly dependent row in the stoichiometry matrix $\mathbf{N}$. We follow the procedure and terminology described by Reder [54] (see also [26]) in the reduction of the system.

Let n_0 denote the row rank of $\mathbf{N}$. If $n_0 = n$, then no reduction is necessary. Otherwise, we begin by re-ordering the rows of $\mathbf{N}$ so that the first n_0 rows are linearly independent. Let $\mathbf{N_R}$ be the reduced stoichiometry matrix which results from truncating the last $n - n_0$ rows of $\mathbf{N}$. Since the truncated rows can be formed by linear combination of the rows of $\mathbf{N_R}$, the matrix $\mathbf{N}$ can be written as the product

$$\mathbf{N} = \mathbf{L}\mathbf{N_R}$$

where the $n \times n_0$ matrix $\mathbf{L}$, called the *link matrix*, has the form

$$\mathbf{L} = \begin{bmatrix} \mathbf{I}_{n_0} \\ \mathbf{L_0} \end{bmatrix}.$$

(Here and below the notation $\mathbf{I}_q$ will be used for the $q \times q$ identity matrix).

The advantage of this decomposition can now be realized. Since each structural conservation allows one species concentration to be determined as a function of the others, we may decompose the species vector $\mathbf{s}$ into an independent species vector $\mathbf{s}_i$ and a dependent species vector $\mathbf{s}_d$. Ordering the components of $\mathbf{s}$ to match the rows of $\mathbf{N}$, we write $\mathbf{s} = (\mathbf{s}_i, \mathbf{s}_d)$ where $\mathbf{s}_i$ is an n_0-tuple and $\mathbf{s}_d$ is an $(n - n_0)$-tuple. (This involves a minor abuse of notation since $\mathbf{s}$, $\mathbf{s}_i$ and $\mathbf{s}_d$ are all column vectors.) Then equation (1) can be written as

$$\frac{d}{dt}\begin{bmatrix} \mathbf{s}_i(t) \\ \mathbf{s}_d(t) \end{bmatrix} = \mathbf{L}\mathbf{N_R}\mathbf{v}(\mathbf{s}(t), \mathbf{p}, t) = \begin{bmatrix} \mathbf{I}_{n_0} \\ \mathbf{L_0} \end{bmatrix} \mathbf{N_R}\mathbf{v}(\mathbf{s}(t), \mathbf{p}, t) \qquad \text{for all } \ t \geq 0.$$

Hence

$$\frac{d}{dt}\mathbf{s}_d(t) = \mathbf{L_0}\frac{d}{dt}\mathbf{s}_i(t) \qquad \text{for all } \ t \geq 0,$$

and so $\mathbf{s}_d(t) - \mathbf{L_0}\mathbf{s}_i(t)$ is an integral of motion of (1), i.e. this difference is constant throughout the evolution of the system. We introduce the constant $(n - n_0)$-vector $\mathbf{T}$ to quantify this relationship. Any trajectory of the system satisfies

$$\mathbf{s}_d(t) = \mathbf{L_0}\mathbf{s}_i(t) + \mathbf{T} \qquad \text{for all } \ t \geq 0, \tag{2}$$

where $\mathbf{T}$ is defined in terms of the initial conditions as

$$\mathbf{T} = \mathbf{s}_d(0) - \mathbf{L_0}\mathbf{s}_i(0).$$

In analysis and computation, attention can be restricted to the independent species $\mathbf{s}_i$, since the corresponding results incorporating the dependent vector $\mathbf{s}_d$ are arrived at immediately through the relationship (2). That is, one need only consider the reduced system

$$\frac{d}{dt}\mathbf{s}_i(t) = \mathbf{N_R}\mathbf{v}(\mathbf{s}(t),\mathbf{p},t) = \mathbf{N_R}\mathbf{v}((\mathbf{s}_i(t),\mathbf{L_0}\mathbf{s}_i(t)+\mathbf{T}),\mathbf{p},t) \qquad \text{for all } \ t \geq 0. \tag{3}$$

Local analysis of system (3) will be carried out in the neighbourhood of a steady state $(\mathbf{s}_i^0,\mathbf{p}^0)$ of interest. This point is brought to the origin by a change of variables in the states: $\mathbf{x}(t) = \mathbf{s}_i(t) - \mathbf{s}_i^0$, and in the parameters: $\mathbf{u}(t) = \mathbf{p}(t) - \mathbf{p}^0$. The n-vector $\mathbf{x}$ and the m-vector $\mathbf{u}$ indicate the deviation from the nominal state and parameter values of (3), respectively. The linearized system then takes the form

$$\dot{\mathbf{x}}(t) = \left[\mathbf{N_R}\frac{\partial \mathbf{v}}{\partial \mathbf{s}}\mathbf{L}\right]\mathbf{x}(t) + \left[\mathbf{N_R}\frac{\partial \mathbf{v}}{\partial \mathbf{p}}\right]\mathbf{u}(t), \tag{4}$$

where the derivatives are taken at $(\mathbf{s}^0,\mathbf{p}^0) := (\mathbf{L}\mathbf{s}_i^0 + \mathbf{T},\mathbf{p}^0)$. By construction, this linearized system has steady state $(\mathbf{x},\mathbf{u}) = (\mathbf{0},\mathbf{0})$.

The behaviour of the original system (3) is approximated by the behaviour of the linearized system (4) near the nominal operating point. In particular, the linearized model faithfully represents the response of the original system to small changes in the parameters (i.e. functions $\mathbf{u}(\cdot)$ which remain near zero). Standard sensitivity analysis involves gauging the response of system (4) to *constant* (i.e. step) changes in the parameter levels. In extending this analysis to nonconstant perturbations, it is useful to introduce the notations used in systems and control theory for analysing such systems.

1.3 Metabolic Control Analysis

To address the asymptotic response of the system to parameter perturbation, we consider the equation which describes the steady state

$$\mathbf{0} = \mathbf{N}\mathbf{v}(\mathbf{s},\mathbf{p}). \tag{5}$$

Taking a nominal value $\mathbf{p}_0$ for the vector of parameters $\mathbf{p}$, we solve for the corresponding steady state $\mathbf{s}_0$. Provided that the system Jacobian ($\mathbf{N}\frac{\partial \mathbf{v}}{\partial \mathbf{s}}$) is nonsingular, equation (5) defines $\mathbf{s}$ as an implicit function of $\mathbf{p}$. We write $\mathbf{s} = \mathbf{s}(\mathbf{p})$, with $\mathbf{s}(\mathbf{p}_0) = \mathbf{s}_0$. The assumption of nonsingularity is standard (see e.g. [54]), in particular, it holds whenever $\mathbf{s}_0$ is an asymptotically stable steady state, which is the only case the will be experimentally observed.

The response of the steady state $\mathbf{s}_0$ to perturbations in the parameter values can be approximated by the sensitivity of the function $\mathbf{s}(\mathbf{p})$ to changes in its argument, i.e. by the derivative $\frac{d\mathbf{s}}{d\mathbf{p}}$. This linear approximation is accurate for small paramter perturbations, but in general will be less accurate as the size of the perturbation grows.

Calculating, we find

$$0 = \frac{d}{d\mathbf{p}}\mathbf{N}\mathbf{v}(\mathbf{s}(\mathbf{p}),\mathbf{p}) = \mathbf{N_R}\left[\frac{\partial \mathbf{v}}{\partial \mathbf{s}}\mathbf{L}\frac{d\mathbf{s}_i}{d\mathbf{p}} + \frac{\partial \mathbf{v}}{\partial \mathbf{p}}\right],$$

where the derivatives are evaluated at $\mathbf{s} = \mathbf{s}_0$, $\mathbf{p} = \mathbf{p}_0$. Under our standing assumption that $\mathbf{N_R}\frac{\partial \mathbf{v}}{\partial \mathbf{s}}\mathbf{L}$ is invertible, we find the sensitivity,

$$\frac{d\mathbf{s}_i(\mathbf{p})}{d\mathbf{p}} = -\left(\mathbf{N_R}\frac{\partial \mathbf{v}}{\partial \mathbf{s}}\mathbf{L}\right)^{-1}\mathbf{N_R}\frac{\partial \mathbf{v}}{\partial \mathbf{p}}.$$

Sensitivitites of the dependent species follow from (2).

In addition to the sensitivity of the species levels we are also interested in the response of the steady state fluxes through the network to changes in $\mathbf{p}$. These fluxes are determined by the steady state reaction rates. Considering the response in the steady state rate vector we find

$$\begin{aligned}\frac{d\mathbf{v}(\mathbf{s}(\mathbf{p}),\mathbf{p})}{d\mathbf{p}} &= \frac{\partial \mathbf{v}}{\partial \mathbf{s}}\frac{d\mathbf{s}}{d\mathbf{p}} + \frac{\partial \mathbf{v}}{\partial \mathbf{p}} \\ &= \frac{\partial \mathbf{v}}{\partial \mathbf{s}}\mathbf{L}\frac{d\mathbf{s}_i}{d\mathbf{p}} + \frac{\partial \mathbf{v}}{\partial \mathbf{p}} \\ &= -\frac{\partial \mathbf{v}}{\partial \mathbf{s}}\mathbf{L}\left(\mathbf{N_R}\frac{\partial \mathbf{v}}{\partial \mathbf{s}}\mathbf{L}\right)^{-1}\mathbf{N_R}\frac{\partial \mathbf{v}}{\partial \mathbf{p}} + \frac{\partial \mathbf{v}}{\partial \mathbf{p}}.\end{aligned}$$

1.3.1 Definitions

In MCA the system sensitivities derived above are known as the system *responses*. We follow [54, 26], in making the following definition.

Definition 1.1 Given a nominal parameter value $\mathbf{p}_0$ and a corresponsing steady state $\mathbf{s}_0$ of system (1), the independent *concentration response coefficients* are defined as the elements of the *n* by *r* matrix

$$\mathbf{R^{s_i}} := \frac{d\mathbf{s}_i(\mathbf{p})}{d\mathbf{p}} = -\left(\mathbf{N_R}\frac{\partial \mathbf{v}}{\partial \mathbf{s}}\mathbf{L}\right)^{-1}\mathbf{N_R}\frac{\partial \mathbf{v}}{\partial \mathbf{p}}.$$

The *rate response coefficients* are defined similarly as the elements of the *m* by *r* matrix

$$\mathbf{R^v} := \frac{d\mathbf{v}(\mathbf{s}(\mathbf{p}),\mathbf{p})}{d\mathbf{p}} = -\left\{\frac{\partial \mathbf{v}}{\partial \mathbf{s}}\mathbf{L}\left(\mathbf{N_R}\frac{\partial \mathbf{v}}{\partial \mathbf{s}}\mathbf{L}\right)^{-1}\mathbf{N_R} + \mathbf{I}_m\right\}\frac{\partial \mathbf{v}}{\partial \mathbf{p}}.$$

□

A traditional MCA presentation would also treat the special case of response coefficients in the case that $\frac{\partial \mathbf{v}}{\partial \mathbf{p}} = \mathbf{I}$. These expressions, called *control coefficients*, indicate the sensitivity of the system to perturbations in the reaction rates themselves.

The partial derivatives of the rate function $\mathbf{v}(\cdot,\cdot)$ are also given special names in MCA, as follows.

Definition 1.2 The *species elasticity* $\varepsilon_\mathbf{s}$ and *parameter elasticity* $\varepsilon_\mathbf{p}$ are defined as

$$\varepsilon_\mathbf{s} := \frac{\partial \mathbf{v}}{\partial \mathbf{s}} \qquad \varepsilon_\mathbf{p} := \frac{\partial \mathbf{v}}{\partial \mathbf{p}}.$$

□

One of the major successes of MCA was the derivation of the systemic response coefficients from these component-specific elasticities (which are often more amenable to experimental measurment). This was originally achieved through the Summation and Connectivity Theorems. However, as was shown by Reder [54], the systemic response can be *defined* as a function of the elasticities (as above) without any reference to the Theorems. The Summation and Connectivity relations are then used to provide further insight into the system's behaviour.

1.3.2 The Summation and Connectivity Theorems

The MCA theorems can be stated as algebraic conditions satisfied by the control coefficients and elasticities (see, e.g. [54, 26]). As in [33], they will be presented here as properties of the system response coefficients. In each case, we consider the choice of the parameter $\mathbf{p}$ as part of the hypothesis. That is, given a particular system, we ask what sort of responses might be achieved by singling out a particular parameter $\mathbf{p}$.

Proposition 1.3 (Connectivity Theorem) If a parameter is chosen so that $\varepsilon_{\mathbf{p}} = \frac{\partial \mathbf{v}}{\partial \mathbf{p}}$ is in the span of the columns of $\varepsilon_{\mathbf{s}}\mathbf{L}$, then there exists an r-vector $\mathbf{m}$ so that $\varepsilon_{\mathbf{p}} = -\varepsilon_{\mathbf{s}}\mathbf{L}\mathbf{m}$ (note the minus) and

$$\mathbf{R}^{\mathbf{s_i}} = \mathbf{m} \qquad \text{and} \qquad \mathbf{R}^{\mathbf{v}} = \mathbf{0}.$$

Proposition 1.4 (Summation Theorem) If a parameter is chosen such that $\varepsilon_{\mathbf{p}} = \frac{\partial \mathbf{v}}{\partial \mathbf{p}}$ lies in the nullspace of $\mathbf{N}$, then

$$\mathbf{R}^{\mathbf{s_i}} = \mathbf{0} \qquad \text{and} \qquad \mathbf{R}^{\mathbf{v}} = \frac{\partial \mathbf{v}}{\partial \mathbf{p}}.$$

In both cases the proof is an exercise in matrix multiplication.

The dual nature of the results is apparent. The first describes conditions in which parameters variation leads to changes in species concentrations while steady state reaction rates do not vary. The second indicates conditions under which perturbations have the exact opposite effect.

1.4 Input-Output Systems

The standard model of a linear time-invariant input-output system has the form

$$\dot{\mathbf{x}}(t) = \mathbf{A}\mathbf{x}(t) + \mathbf{B}\mathbf{u}(t) \qquad \text{for all } t \geq 0, \tag{6}$$

where $\mathbf{x}$ is an n-vector, $\mathbf{u}(t)$ is an m-vector, and $\mathbf{A}$ and $\mathbf{B}$ are matrices of dimension $n \times n$ and $n \times m$ respectively. The linearized model (4) takes this form with

$$\mathbf{A} = \mathbf{N}_{\mathbf{R}} \left.\frac{\partial \mathbf{v}}{\partial \mathbf{s}}\mathbf{L}\right|_{\mathbf{s}=\mathbf{s}^0,\mathbf{p}=\mathbf{p}^0} \qquad \text{and} \qquad \mathbf{B} = \mathbf{N}_{\mathbf{R}} \left.\frac{\partial \mathbf{v}}{\partial \mathbf{p}}\right|_{\mathbf{s}=\mathbf{s}^0,\mathbf{p}=\mathbf{p}^0}.$$

The components of the *input* vector $\mathbf{u}$ can play a number of roles in the system. In control engineering, three of the most common are: reference input, control input, and disturbance.

A *reference input* provides an external signal which the system is expected to track. This reference could be either constant (e.g. the set-point of a thermostat) or time-varying (e.g. the prescribed trajectory of a missile). The input to information-processing systems often plays such a role. For example, ligand-binding is a reference input for many signal transduction networks – the associated cellular activity should track the ligand level in an appropriate manner.

A *control* is an input which is manipulable in some way. System design typically leads to *feedback laws* acting through control channels, whereby the control input is chosen as a function of the state: $\mathbf{u}(t) = \mathbf{k}(\mathbf{x}(t))$. In biochemical systems, experimentally manipulable parameters can be considered as control inputs. A more subtle analogy comes from the conceptual division of systems into subnetworks acting on one another. For example, thinking of the influence of genetic networks on metabolism as the action of a controller on a system, one can ask what measure of authority the controlling system possesses and what sort of feedbacks have been implemented.

A *disturbance input* can be included in the model as an attempt to incorporate the effect of external perturbations on the system. Engineers typically design systems with these effects in mind; control laws are chosen based on their ability to attenuate the effect of harmful disturbances. The ability of biochemical networks to continue their function in the presence of perturbations is a central feature of life. This homeostatic regulation is achieved through the appropriate use of feedback control.

In system analysis and design, it is often the case that certain functions of the state and input are of specific interest. These are defined as the system *outputs*. A common example is an output consisting of a single component of the state vector, e.g. the concentration of a particular molecular species. In the linear systems framework, an output vector $\mathbf{y}$ is included by appending the definition

$$\mathbf{y}(t) = \mathbf{C}\mathbf{x}(t) + \mathbf{D}\mathbf{u}(t) \tag{7}$$

to (6), where $\mathbf{C}$ and $\mathbf{D}$ are matrices of appropriate dimensions.

In addressing biochemical systems, there are several outputs which may be of interest, including species concentrations, reaction rates, pathway fluxes, transient times, and rates of entropy production (cf. section 5.8.1 of [25]). In what follows, two output vectors of primary interest will be addressed.

The first is the vector of independent species concentrations, or more precisely, the deviations of these concentrations from the nominal level. In the linearized model (4), these deviations are described by the state $\mathbf{x}$. This choice of output is thus characterized by

$$\mathbf{y}(t) = \mathbf{x}(t),$$

which is (7) with $\mathbf{C} = \mathbf{I}$ (the $n \times n$ identity matrix) and $\mathbf{D} = \mathbf{0}$.

The second output of interest is the vector of reaction rates. Again, it is the deviation from the nominal rates which is the natural choice for $\mathbf{y}$. This is approximated by the linearization of the reaction rate function $\mathbf{v}(\cdot,\cdot)$ at the nominal point as follows:

$$\mathbf{y}(t) = \frac{\partial \mathbf{v}}{\partial \mathbf{s}}\mathbf{L}\mathbf{x}(t) + \frac{\partial \mathbf{v}}{\partial \mathbf{p}}\mathbf{u}(t),$$

where the derivatives are evaluated at $(\mathbf{s}^0, \mathbf{p}^0)$. This output takes the form of (7) with $\mathbf{C} = \frac{\partial \mathbf{v}}{\partial \mathbf{s}}\mathbf{L}$ and $\mathbf{D} = \frac{\partial \mathbf{v}}{\partial \mathbf{p}}$.

1.5 Frequency Response

Sensitivity analysis is concerned with determining the steady state response of a system to *constant* (i.e. step) disturbances, e.g. an instantaneous change in the activity of an enzyme from one constant level to another. Extending that analysis to determination of the asymptotic response to arbitrary time-varying perturbations may seem a daunting task. Indeed, this is an intractable problem in general. However, when restricting to linear systems, a satisfactory result can be achieved.

There are two features of linear systems which allow this analysis. The first is simply the linear nature of their input-output behaviour which implies an *additive property*: provided the system starts with initial condition $\mathbf{x}(0) = \mathbf{0}$ (which corresponds to the nominal steady state of the biochemical network), the output produced by the sum of two inputs is the sum of the outputs produced independently by the two inputs. That is, if input $\mathbf{u}_1(\cdot)$ elicits output $\mathbf{y}_1(\cdot)$ and input $\mathbf{u}_2(\cdot)$ yields output $\mathbf{y}_2(\cdot)$, then input $\mathbf{u}_1(\cdot) + \mathbf{u}_2(\cdot)$ leads to output $\mathbf{y}_1(\cdot) + \mathbf{y}_2(\cdot)$.

The additive property allows a reductionist approach to the analysis of system response: if a complicated input can be written as a sum of simpler signals, the response to each of these simpler inputs can

be addressed separately, and the original response can be found through a straightforward summation. This leads to a satisfactory procedure provided one is able to find a family of "simple" functions with the following two properties: 1) the family has to be "complete" in the sense that an arbitrary signal can be decomposed into a sum of functions chosen from this family; and 2) it must enjoy the property that the asymptotic response of a linear system to inputs chosen from the family is easily characterized. The family of sinusoids (sines and cosines) satisfies both of these conditions.

That the set of sinusoids is sufficiently rich to allow any function to be written as a combination of these functions was recognized by Fourier in the early 19th century and is a cornerstone of the theory of signal processing (cf. e.g. [44, 65]). In general, if a function $f(t)$ is periodic with period 2π, then one can write

$$f(t) = a_0 + a_1\cos(t) + b_1\sin(t) + a_2\cos(2t) + b_2\sin(2t) + \cdots,$$

where

$$a_k = \frac{1}{\pi}\int_{-\pi}^{\pi} f(t)\cos(kt)\,dt \qquad \text{and} \qquad b_k = \frac{1}{\pi}\int_{-\pi}^{\pi} f(t)\sin(kt)\,dt.$$

Figures 1-4 illustrate the case where $f(t)$ is a square-wave. The Figures show the improvement in approximation as more terms are added to the sum. That these coefficients can be found so readily is a consequence of the *orthogonality* of the family of sinusoids. A more concise decomposition can be reached by expressing the sinusoids in terms of exponentials through

$$\cos(t) = \frac{1}{2}(e^{it} + e^{-it}) \qquad \text{and} \qquad \sin(t) = \frac{-i}{2}(e^{it} - e^{-it})$$

where $i = \sqrt{-1}$. Rewriting in this form leads to the decomposition

$$f(t) = \sum_{k=-\infty}^{\infty} c_k e^{ikt} \qquad \text{where} \qquad c_k = \frac{1}{2\pi}\int_{-\pi}^{\pi} f(t)e^{-ikt}\,dt. \tag{8}$$

Such a decomposition allows an alternative characterization of the function $f(\cdot)$ in terms of the list of Fourier coefficients $\ldots, c_{-2}, c_{-1}, c_0, c_1, c_2, \ldots$. These coefficients describe the *frequency content* (or *spectrum*) of the function, recording the "density" of the corresponding sinusoid within the signal $f(t)$.

Functions which are not periodic demand an extended analysis since they cannot be expressed as a sum of sines and cosines at discrete frequencies. Such functions can only be expressed as a combination of sinusoids by allowing components at all frequencies. The discrete list of frequency content is thus extended to a function $F(\omega)$ which describes the content at each frequency ω. This function is known as the Fourier integral or *Fourier transform*. The continuum of components expressed in $F(\omega)$ can be "summed" by integration to yield the original function $f(t)$ as follows,

$$f(t) = \int_{-\infty}^{\infty} F(\omega)e^{i\omega t}\,d\omega \qquad \text{where} \qquad F(\omega) = \frac{1}{2\pi}\int_{-\infty}^{\infty} f(t)e^{-i\omega t}\,dt. \tag{9}$$

The analogy between (8) and (9) is immediate.

In both cases the record of the frequency content of the function (i.e. the transform) is an alternative characterization of the original function. While complete recovery of a signal from its transform involves computation of the integral on the left-hand side of (9), important aspects of the nature of the signal can be gleaned directly from the graph of the transform. In particular, one can determine what sort of variations dominate the signal (e.g. low frequency or high frequency). As an example, consider the functions $f(t) = \frac{1}{1+t^2}$ and $g(t) = \cos(4t)\frac{1}{1+t^2}$ shown in Fig. 5. These functions share the same basic

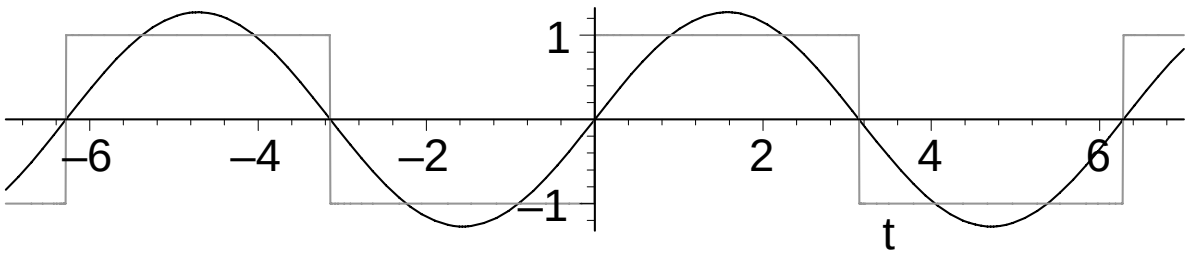

Fig. 1: $\frac{4}{\pi}\sin(t)$

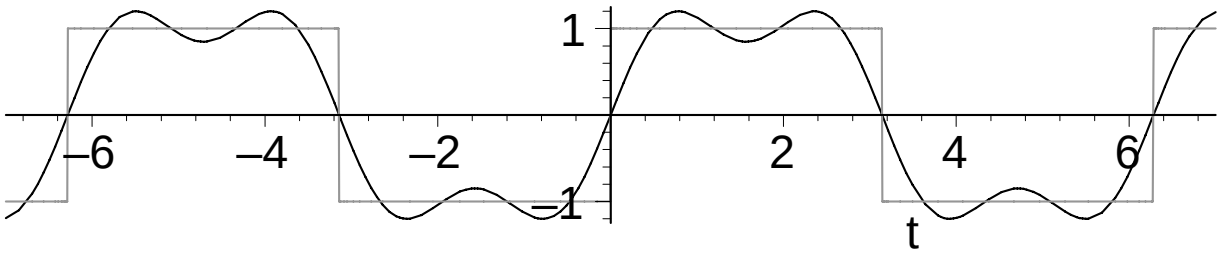

Fig. 2: $\frac{4}{\pi}\left(\sin(t)+\frac{\sin(3t)}{3}\right)$

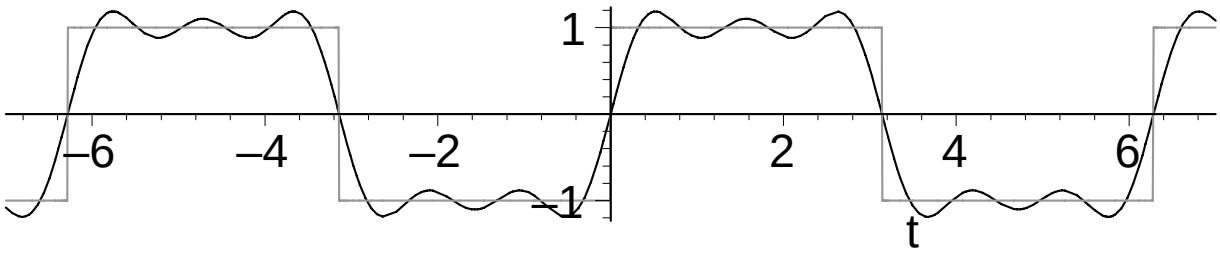

Fig. 3: $\frac{4}{\pi}\left(\sin(t)+\frac{\sin(3t)}{3}+\frac{\sin(5t)}{5}\right)$

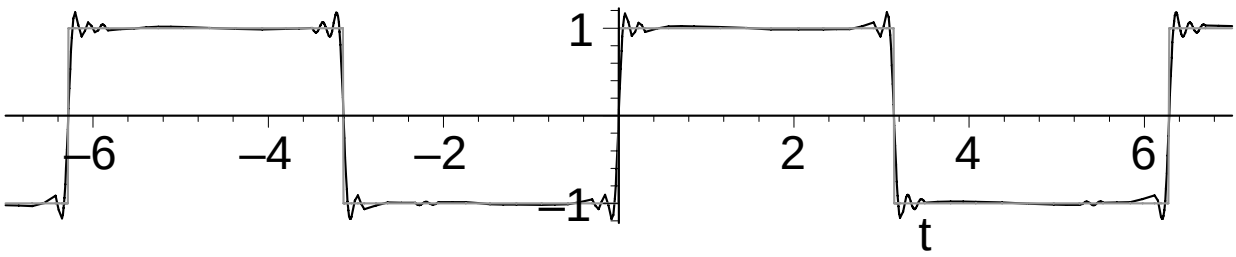

Fig. 4: $\frac{4}{\pi}\sum_{n=1}^{20}\frac{\sin(2n-1)t}{2n-1}$

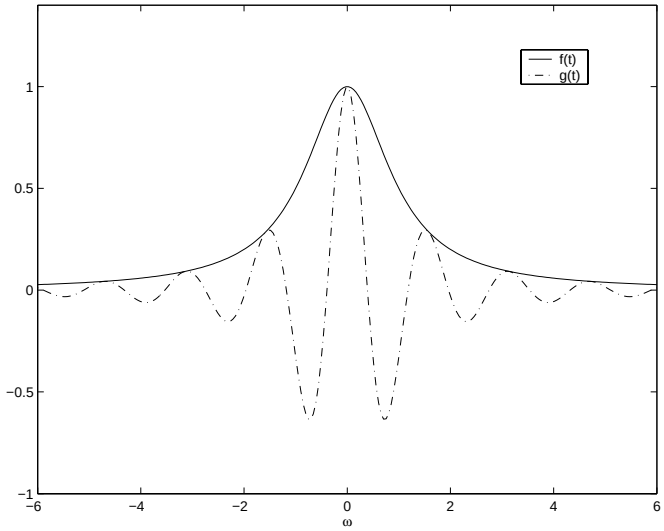

Fig. 5: Functions $f(t) = \frac{1}{1+t^2}$ and $g(t) = \cos(4t)\frac{1}{1+t^2}$

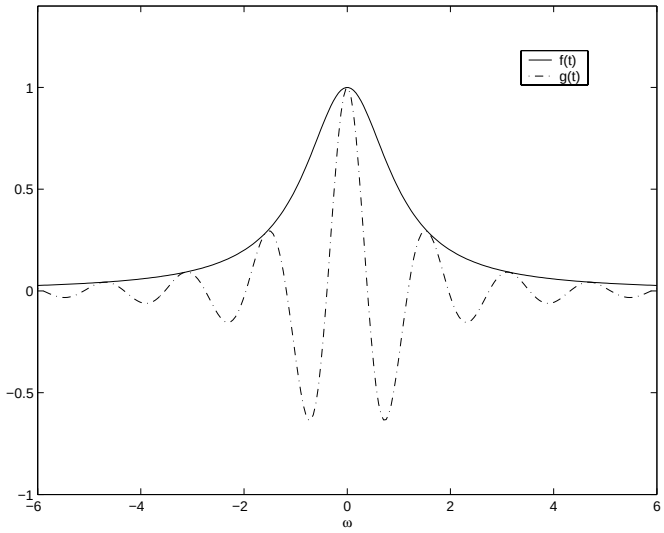

Fig. 6: Fourier Transforms of $f(t)$ and $g(t)$

"profile". However, $f(t)$ follows a slowly varying path, while $g(t)$ varies much more rapidly. This difference in their nature is evident in comparison of their Fourier transforms, shown in Fig. 6. The transform of $f(\cdot)$ is dominated by content at near-zero frequencies (corresponding to slowly varying sinusoids) while the content of $g(\cdot)$ is concentrated at $\omega = 4$, which is the frequency of its quasi-periodic behaviour. (The introduction of "negative frequencies" is a consequence of the exponential description of the sinusoids. The symmetry of the transform allows attention to be restricted to positive values of ω in what follows.)

Now that it has been shown that any function can be decomposed into sinusoids, and that linearity can be used to exploit such a decomposition, one question still remains. How is it that the response of a system to these "simple" sinusoidal inputs can be recorded in a useful way? After all, the procedure outlined above demands that one "sum" over a continuum of responses to arrive at the response to a given signal. This will only be a useful strategy if the "simple" responses are easily characterized. The second crucial property of linear systems which will be used is that, as mentioned above, their response to sinusoidal inputs can be very easily described. (Indeed, it is this property of sines and cosines which makes Fourier analysis a useful tool for analysing linear time-invariant systems. There are many other complete and orthogonal families of functions into which one can decompose arbitrary signals as described above, but only the sinusoids produce appropriately convenient outputs from linear systems. The widespread use of Fourier analysis by electrical engineers is not due to the ubiquity of alternating (i.e. oscillatory) electrical signals but rather to mathematical necessity.)

Consider the case of a system for which the input and output are scalars, referred to as Single-Input-Single-Output (SISO) systems. For such systems, an oscillatory input elicits an asymptotic response which can be characterized by just two numbers. More precisely, the output of a linear SISO system whose input is a sinusoid of frequency ω tends asymptotically to a sinusoid of frequency ω. That is, an oscillatory input of the form $u(t) = e^{i\omega t}$ produces an output $y(t)$ which converges asymptotically to $Ae^{i\omega t+\phi}$. This asymptotic response can be described by two numbers: A, the amplitude of the oscillatory output, known as the *system gain*; and ϕ, the phase of the oscillatory output, known as the *phase shift*. For systems which are not SISO, there is one such pair of numbers which characterizes the response of each output "channel" (i.e. component) to each input channel. In the current discussion, this extension is simply a matter of bookkeeping.

The conclusion of this discussion is that the behaviour of the system can be completely described by the values of the gain A and phase shift ϕ at each frequency ω. These two numbers can be conveniently described in terms of a single complex number $Ae^{i\phi}$ with modulus A and argument ϕ. The system, then, can be characterized by a complex-valued function defined over all frequencies. This function, called the *frequency response* of the system can be derived through an algebraic calculation involving the Laplace transform of the system, cf. e.g. [48]. (The Laplace transform is an extension of the Fourier transform, see e.g. [65]). The frequency response for system (6) with output given by (7) is

$$\mathbf{H}(i\omega) = \mathbf{C}(i\omega\mathbf{I} - \mathbf{A})^{-1}\mathbf{B} + \mathbf{D}, \qquad \text{for all real } \omega.$$

This function will in general be matrix-valued but is scalar-valued in the SISO case. The frequency response is usually derived as the restriction of a function of a complex variable z to the imaginary axis. The complete function $\mathbf{H}(z)$ is known as the *transfer function* of the system.

Considering the two outputs of interest indicated above, the corresponding frequency response functions are found as follows. For the independent species concentration output, we have $\mathbf{C} = \mathbf{I}$ and $\mathbf{D} = \mathbf{0}$, and so the frequency response takes the form

$$\mathbf{H}_{s_i}(i\omega) = (i\omega\mathbf{I} - \mathbf{N_R}\frac{\partial \mathbf{v}}{\partial \mathbf{s}}\mathbf{L})^{-1}\mathbf{N_R}\frac{\partial \mathbf{v}}{\partial \mathbf{p}}. \tag{10}$$

For the reaction rate output, $\mathbf{C} = \frac{\partial \mathbf{v}}{\partial \mathbf{s}}\mathbf{L}$ and $\mathbf{D} = \frac{\partial \mathbf{v}}{\partial \mathbf{p}}$ give

$$\mathbf{H}_v(i\omega) = \frac{\partial \mathbf{v}}{\partial \mathbf{s}}\mathbf{L}(i\omega\mathbf{I} - \mathbf{N_R}\frac{\partial \mathbf{v}}{\partial \mathbf{s}}\mathbf{L})^{-1}\mathbf{N_R}\frac{\partial \mathbf{v}}{\partial \mathbf{p}} + \frac{\partial \mathbf{v}}{\partial \mathbf{p}}. \tag{11}$$

These expressions define matrix-valued frequency responses of systems which have multiple output and input channels. Each element of such a matrix-valued function is a scalar-valued function which describes the response of one output channel to one input channel. For each such input/output channel pair, the complex-valued function which describes the system behaviour can be plotted in a number of ways. Perhaps the most useful of these visualizations is the *Bode plot*, in which the magnitude and argument of the frequency response are plotted separately. The magnitude of the function value (the system gain) is plotted on a log-log scale, where the gain is measured in decibels (dB) (defined by x dB = $20\log_{10} x$). The argument of the function value (the phase shift) appears on a semi-log plot, with log frequency plotted against phase in degrees. Examples of Bode plots are shown in Section 6.

The response of a system to a constant input (which can be thought of as a sinusoid with frequency zero) is characterized by the frequency response at $\omega = 0$. Making this substitution into (10),(11) the response of the system is found as

$$\mathbf{H}_{s_i}(0) = -(\mathbf{N_R}\frac{\partial \mathbf{v}}{\partial \mathbf{s}}\mathbf{L})^{-1}\mathbf{N_R}\frac{\partial \mathbf{v}}{\partial \mathbf{p}} \qquad \text{and} \qquad \mathbf{H}_v(0) = -\frac{\partial \mathbf{v}}{\partial \mathbf{s}}\mathbf{L}(\mathbf{N_R}\frac{\partial \mathbf{v}}{\partial \mathbf{s}}\mathbf{L})^{-1}\mathbf{N_R}\frac{\partial \mathbf{v}}{\partial \mathbf{p}} + \frac{\partial \mathbf{v}}{\partial \mathbf{p}}. \tag{12}$$

These expressions can be derived from a standard sensitivity analysis of system (3). A framework for such an analysis is provided by MCA, which is addressed in the next section.

1.6 Metabolic Control Analysis in the Frequency Domain

The expressions of system sensitivity in (12) are *response coefficients* in MCA. This definition can be generalized to address the entire frequency response as follows.

Definition 1.5 The (frequency dependent) unscaled *concentration response coefficients* of system (3) are the elements of the matrix function

$$\mathbf{R}_{s_i}(\omega) := \mathbf{H}_s(i\omega) = (i\omega\mathbf{I} - \mathbf{N_R}\frac{\partial \mathbf{v}}{\partial \mathbf{s}}\mathbf{L})^{-1}\mathbf{N_R}\frac{\partial \mathbf{v}}{\partial \mathbf{p}}. \tag{13}$$

The (frequency dependent) unscaled *rate response coefficients* of system (3) are the elements of

$$\mathbf{R}_v(\omega) := \mathbf{H}_v(i\omega) = \frac{\partial \mathbf{v}}{\partial \mathbf{s}}\mathbf{L}(i\omega\mathbf{I} - \mathbf{N_R}\frac{\partial \mathbf{v}}{\partial \mathbf{s}}\mathbf{L})^{-1}\mathbf{N_R}\frac{\partial \mathbf{v}}{\partial \mathbf{p}} + \frac{\partial \mathbf{v}}{\partial \mathbf{p}}. \tag{14}$$

Further, define the (frequency dependent) unscaled *concentration control coefficients* and *rate control coefficients* as the elements of

$$\mathbf{C}_{s_i}(\omega) = (i\omega\mathbf{I} - \mathbf{N_R}\frac{\partial \mathbf{v}}{\partial \mathbf{s}}\mathbf{L})^{-1}\mathbf{N_R} \qquad \text{and} \qquad \mathbf{C}_v(\omega) = \frac{\partial \mathbf{v}}{\partial \mathbf{s}}\mathbf{L}(i\omega\mathbf{I} - \mathbf{N_R}\frac{\partial \mathbf{v}}{\partial \mathbf{s}}\mathbf{L})^{-1}\mathbf{N_R} + \mathbf{I}. \tag{15}$$

□

These response coefficients exhibit the frequency response of the system. For nonzero frequency ω, these coefficients will in general be complex-valued, describing both the gain and the phase shift of the system response.

The definitions given above describe unscaled sensitivities, as opposed to the more commonly used scaled sensitivities of MCA. This "scaling" refers to the the treatment of relative, rather than absolute, sensitivities. These relative sensitivities can be recovered from the definitions above through multiplication by a scaling factor. To that end, define the diagonal matrices

$$\mathbf{D}^{s_i} = \text{diag}\,[\mathbf{s}_i^0] \qquad \mathbf{D}^v = \text{diag}\,[\mathbf{v}(\mathbf{s}^0, \mathbf{p}^0)] \qquad \mathbf{D}^p = \text{diag}\,[\mathbf{p}^0],$$

as in [26]. The scaled response coefficients describing the relative sensitivities are then given by

$$\widetilde{\mathbf{R}}_{s_i}(\omega) = [\mathbf{D}^{s_i}]^{-1}\mathbf{R}_{s_i}(\omega)\mathbf{D}^p \qquad\qquad \widetilde{\mathbf{R}}_v(\omega) = [\mathbf{D}^v]^{-1}\mathbf{R}_v(\omega)\mathbf{D}^p$$

where the tilde ($\sim$) denotes the scaled coefficient. Scaled control coefficients are defined similarly.

1.6.1 MCA Theorems

The stoichiometric nature of a biochemical system enforces certain relations on the sensitivities of the system with respect to parameter perturbations. For step perturbations, such relations are described by the Summation and Connectivity Theorems of MCA. These relations can be extended beyond the $\omega = 0$ case to the frequency response defined above. These generalized Theorems are stated below as algebraic conditions involving the control coefficients, following statements found in [26, 54]. The statements can be translated into results involving scaled coefficients by the appropriate multiplications.

Theorem 1 *:* **Summation Theorem** *If a vector* $\mathbf{k}$ *lies in the nullspace of* $\mathbf{N_R}$ *(and hence of* $\mathbf{N}$*), then*

$$\mathbf{C}_{s_i}(\omega)\mathbf{k} = \mathbf{0} \qquad \textit{and} \qquad \mathbf{C}_v(\omega)\mathbf{k} = \mathbf{k}$$

for all $\omega \geq 0$*.* ∎

The statement follows directly from the definition of the control coefficients (15). This result can be interpreted in terms of the system response as follows.

Interpretation: If the vector of parameters $\mathbf{p}$ is chosen so that the columns of $\frac{\partial \mathbf{v}}{\partial \mathbf{p}}$ lie in the nullspace of $\mathbf{N_R}$ then the responses are given by

$$\mathbf{R}_{s_i}(\omega) = 0 \qquad \text{and} \qquad \mathbf{R}_v(\omega) = \frac{\partial \mathbf{v}}{\partial \mathbf{p}}$$

for all $\omega \geq 0$.

This result is immediate from the form of the linearized system (4), since such a parameter $\mathbf{p}$ leads to $\mathbf{B} = \mathbf{N_R}\frac{\partial \mathbf{v}}{\partial \mathbf{p}} = \mathbf{0}$. In this case the species concentrations are completely decoupled from changes in $\mathbf{p}$, leading to the output responses indicated.

Theorem 2 *:* **Connectivity Theorem** *For the control coefficients as described above,*

$$\mathbf{C}_{s_i}(\omega)\frac{\partial \mathbf{v}}{\partial \mathbf{s}}\mathbf{L} = -\mathbf{I} + i\omega(i\omega\mathbf{I} - \mathbf{N_R}\frac{\partial \mathbf{v}}{\partial \mathbf{s}}\mathbf{L})^{-1}$$

and

$$\mathbf{C}_v(\omega)\frac{\partial \mathbf{v}}{\partial \mathbf{s}}\mathbf{L} = i\omega\frac{\partial \mathbf{v}}{\partial \mathbf{s}}\mathbf{L}(i\omega\mathbf{I} - \mathbf{N_R}\frac{\partial \mathbf{v}}{\partial \mathbf{s}}\mathbf{L})^{-1}.$$

∎

The proof is an exercise in matrix algebra.

Interpretation: Note that if the parameter vector $\mathbf{p}$ is chosen so that the columns of $\frac{\partial \mathbf{v}}{\partial \mathbf{p}}$ lie in the span of the columns of $\frac{\partial \mathbf{v}}{\partial \mathbf{s}}\mathbf{L}$, then there exists a matrix $\mathbf{M}$ so that $\frac{\partial \mathbf{v}}{\partial \mathbf{p}} = \frac{\partial \mathbf{v}}{\partial \mathbf{s}}\mathbf{L}\mathbf{M}$. In this case the system response is described by

$$\mathbf{R}_{s_i}(\omega) = [-\mathbf{I} + i\omega(i\omega\mathbf{I} - \mathbf{N}_\mathbf{R}\frac{\partial \mathbf{v}}{\partial \mathbf{s}}\mathbf{L})^{-1}]\mathbf{M} \qquad \text{and} \qquad \mathbf{R}_v(\omega) = i\omega\frac{\partial \mathbf{v}}{\partial \mathbf{s}}\mathbf{L}(i\omega\mathbf{I} - \mathbf{N}_\mathbf{R}\frac{\partial \mathbf{v}}{\partial \mathbf{s}}\mathbf{L})^{-1}\mathbf{M}.$$

This result is not as easy to interpret as that provided by the Summation Theorem. It is insightful, at the least, in the limiting case of low frequency disturbances. For the case $\omega = 0$ the responses are given by

$$\mathbf{R}_{s_i}(0) = -\mathbf{M} \qquad \text{and} \qquad \mathbf{R}_v(0) = \mathbf{0},$$

which agrees with the standard statement of the Connectivity Theorem [26]. Thus for step disturbances (i.e. $\omega = 0$), the Connectivity Theorem provides a result orthogonal to the Summation Theorem in that it indicates which perturbations will affect the species concentrations while leaving the reaction rates unchanged. This conclusion can be extended by observing that for parameters which satisfy the condition above, slowly varying inputs (i.e. consisting of frequencies ω small compared to the eigenvalues of $\mathbf{N}_\mathbf{R}\frac{\partial \mathbf{v}}{\partial \mathbf{s}}\mathbf{L}$) will have only a small effect on the reaction rates.

Considering the form of system (4) provides an immediate derivation of the standard Connectivity Theorem (i.e. the $\omega = 0$ case). Under the condition that $\frac{\partial \mathbf{v}}{\partial \mathbf{p}} = \frac{\partial \mathbf{v}}{\partial \mathbf{s}}\mathbf{L}\mathbf{M}$ the system reduces to

$$\begin{aligned}\dot{\mathbf{x}} &= \left[\mathbf{N}_\mathbf{R}\frac{\partial \mathbf{v}}{\partial \mathbf{s}}\mathbf{L}\right]\mathbf{x} + \left[\mathbf{N}_\mathbf{R}\frac{\partial \mathbf{v}}{\partial \mathbf{s}}\mathbf{L}\right]\mathbf{M}\mathbf{u} \\ &= \left[\mathbf{N}_\mathbf{R}\frac{\partial \mathbf{v}}{\partial \mathbf{s}}\mathbf{L}\right](\mathbf{x} + \mathbf{M}\mathbf{u}).\end{aligned}$$

If $\mathbf{N}_\mathbf{R}\frac{\partial \mathbf{v}}{\partial \mathbf{s}}\mathbf{L}$ is assumed nonsingular, a constant input $\mathbf{u}$ yields a unique steady state of $\mathbf{x} = -\mathbf{M}\mathbf{u}$, corresponding to the form of the species response $\mathbf{R}_{s_i}(0)$. Moreover, in this case the reaction rate output takes the form

$$\mathbf{y} = \frac{\partial \mathbf{v}}{\partial \mathbf{s}}\mathbf{L}(\mathbf{x} + \mathbf{M}\mathbf{u})$$

and so is necessarily zero at steady state.

It can be noted that the limiting case of high frequency oscillations has an interpretation for general perturbations. Considering the definitions of the response coefficients (13), (14), we see that

$$\lim_{\omega\to\infty}\mathbf{R}_{s_i}(\omega) = 0 \qquad \text{and} \qquad \lim_{\omega\to\infty}\mathbf{R}_v(\omega) = \frac{\partial \mathbf{v}}{\partial \mathbf{p}}.$$

These are precisely the responses produced under the Summation Theorem condition that $\mathbf{N}_\mathbf{R}\frac{\partial \mathbf{v}}{\partial \mathbf{p}} = 0$, i.e. no effect on the species concentrations and direct effect on the reaction rates. This response to high-frequency oscillation is characterized by the system's *bandwidth* – the frequency above which the states of the system are insensitive to oscillatory inputs. Perturbations with frequencies above the bandwidth act more quickly than the timescale of the system. Essentially, the state cannot "keep up" with the perturbations, and so reacts only to their average – in this case the zero input.

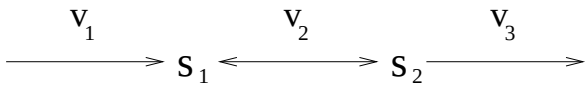

Fig. 7: Simple pathway

1.7 Illustrations of the Frequency Response

The frequency response will now be illustrated by application of the analysis described above to some simple biochemical networks. The first example will be a toy model of an unbranched metabolic chain. This trivial system will serve to demonstrate the Theorems of MCA. Next, simple models of three biological processes will be addressed – tryptophan biosynthesis, glycolysis, and regulation of bacterial chemotaxis. Each of these networks employs a distinct feedback mechanism. The effect of this feedback structure on the system's behaviour will be considered.

1.7.1 Illustration of Theorems: Unbranched Metabolic Pathway

Consider the simple network shown in Fig. 7 with linear kinetics given by

$$\mathbf{v} = \begin{bmatrix} v_1 \\ v_2 \\ v_3 \end{bmatrix} = \begin{bmatrix} k_1 \\ k_2 s_1 - k_{-2} s_2 \\ k_3 s_2 \end{bmatrix}.$$

Thus

$$\frac{\partial \mathbf{v}}{\partial \mathbf{s}} = \begin{bmatrix} 0 & 0 \\ k_2 & -k_{-2} \\ 0 & k_3 \end{bmatrix}$$

The Connectivity Theorem can be illustrated by considering changes in the parameter k_2, as $\mathbf{p} = k_2$ yields

$$\frac{\partial \mathbf{v}}{\partial \mathbf{p}} = \begin{bmatrix} 0 \\ s_1 \\ 0 \end{bmatrix},$$

which is a scalar multiple of the first row of $\frac{\partial \mathbf{v}}{\partial \mathbf{s}}$. (Note $\mathbf{L}$ is the identity matrix in this case.)

With nominal parameter values of

$$k_1 = 6, \quad k_2 = 2, \quad k_{-2} = 1 \text{ and } k_3 = 3,$$

the steady state concentrations are $(s_1^{ss}, s_2^{ss}) = (4,2)$. Setting $\mathbf{x} = (x_1, x_2) = (s_1 - 4, s_2 - 2)$ and $\mathbf{u} = k_2 - 2$, the system can be written in the form (4) as

$$\begin{aligned} \dot{\mathbf{x}}(t) &= \left[\mathbf{N_R}\frac{\partial \mathbf{v}}{\partial \mathbf{s}}\right]\mathbf{x}(t) + \left[\mathbf{N_R}\frac{\partial \mathbf{v}}{\partial \mathbf{p}}\right]\mathbf{u}(t) \\ &= \begin{bmatrix} 1 & -1 & 0 \\ 0 & 1 & -1 \end{bmatrix}\begin{bmatrix} 0 & 0 \\ 2 & -1 \\ 0 & 3 \end{bmatrix}\mathbf{x}(t) + \begin{bmatrix} 1 & -1 & 0 \\ 0 & 1 & -1 \end{bmatrix}\begin{bmatrix} 0 \\ 4 \\ 0 \end{bmatrix}\mathbf{u}(t) \\ &= \begin{bmatrix} -2 & 1 \\ 2 & -4 \end{bmatrix}\mathbf{x}(t) + \begin{bmatrix} -4 \\ 4 \end{bmatrix}\mathbf{u}(t) \end{aligned}$$

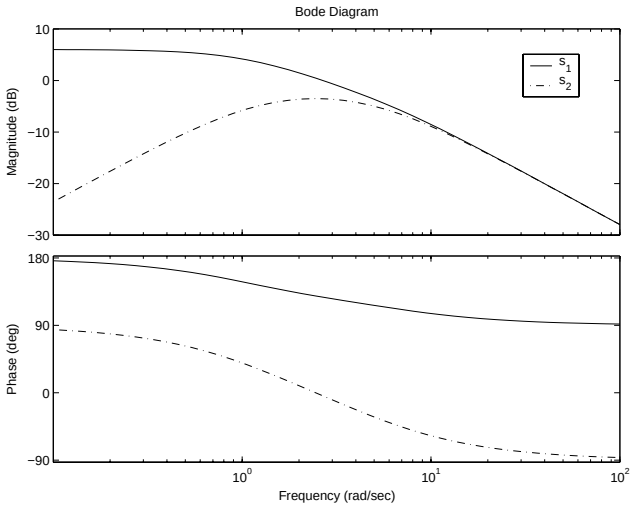

Fig. 8: Bode plot of species concentration response

The asymptotic response of the system to the input $\mathbf{u}(\cdot)$ is described by the Connectivity Theorem. In particular, for a step increase (i.e. $\omega = 0$) there will be a steady-state decrease in s_1 while s_2 and all reaction rates will tend to their nominal steady state values. This result is illustrated by the Bode plots for each of the outputs.

Frequency responses for s_1 and s_2 are shown in Fig. 8 (constructed by choosing $\mathbf{C} = [1 \;\; 0]$, $\mathbf{D} = 0$ and $\mathbf{C} = [0 \;\; 1]$, $\mathbf{D} = 0$, respectively). These plots verify the expected behaviour of the system. For low frequency inputs, the concentration of s_1 responds asymptotically with a 180 degree phase shift and a gain of 6.02 dB. This corresponds to the output being -2 times the input (as -2 has argument 180 degrees in the complex plane, and $20\log_{10} 2 = 6.02$). As described by the Connectivity Theorem, the asymptotic response of s_2 to this input tends to zero at low frequencies (and indeed is zero at $\omega = 0$ though this cannot appear on the log scale). Both species concentrations show a reduced response to high frequency inputs, characterizing the system's bandwidth.

The asymptotic response of the reaction rates is shown in Fig. 9 (found by taking $\mathbf{C} = [2 \;\; -1]$, $\mathbf{D} = 4$ for v_2 as output and $\mathbf{C} = [0 \;\; 3]$, $\mathbf{D} = 0$ for v_3). As the Theorem indicates, the asymptotic response of both reaction rates vanishes as the frequency tends to zero. At high frequencies, the nature of the response is dominated by the "feedthrough" term $\mathbf{D}$, which is 4 (= 12.04 dB) for v_2 and 0 for v_3.

In addition, the Theorems describe the response of the system to two other sets of inputs. The Connectivity Theorem indicates that if k_{-2} and k_3 are perturbed appropriately, the asymptotic response to low frequency inputs will be zero for s_1, v_2 and v_3. This can be easily verified, yielding Bode plots which are similar to those presented above. The coordinated input prescribed by the Theorem can be achieved by replacing k_{-2} with $k_{-2} + \mathbf{u}$ and k_3 with $k_3 + 3\mathbf{u}$ (so any change in k_{-2} is accompanied by a three-fold greater change in k_3).

Finally, the effect of the Summation Theorem can be reached by replacing k_1 with $k_1 + 4\mathbf{u}$, k_2 with $k_2 + \mathbf{u}$ and k_3 with $k_3 + 2\mathbf{u}$. In this case the dynamics are independent of the input, as $\mathbf{B} = \mathbf{0}$. The frequency responses are then constant across all frequencies (0 for species concentrations, 4, 1 and 2 for reactions rates v_1, v_2 and v_3 respectively) as described by the Theorem.

The input-output behaviour of feedback structures will be considered in the next subsections. In each case, it is the gain of the system which is of primary interest, so attention will be restricted to the

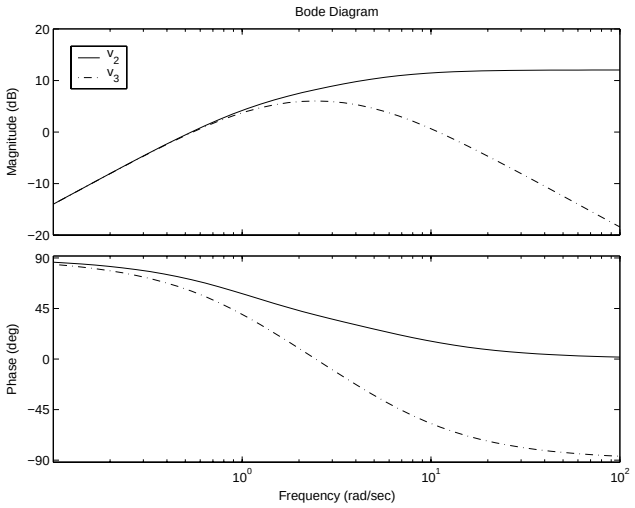

Fig. 9: Bode plot of reaction rate response

magnitude part of the Bode plot. (The phase shift of the system is of major importance in addressing the interconnections of systems, a topic which will not be addressed here).

1.7.2 Negative Feedback: Regulation of Tryptophan Production

The effect of negative feedback on a system will be illustrated by an analysis of the *trp* operon of bacteria, which is responsible for tryptophan production. A number of models of bacterial tryptophan biosynthesis have appeared in the literature, originating with the work of Goodwin [21]. The model of Xiu *et al.* [69] will be considered here. (A more complete model, including explicit time delays, has recently appeared [57].)

The model of Xiu *et al.* involves three state variables: the concentration of tryptophan P; the concentration of mRNA transcribed from the *trp* operon M, and the amount of expressed enzyme E. (It is an abstraction of the model that tryptophan synthesis is catalysed by a single enzyme.) The dynamics of the model describe production of mRNA, enzyme, and tryptophan, as well as the degradation and dilution (due to cell growth) of each of these species. Cellular consumption of tryptophan is also included. In addition, two negative feedbacks are incorporated. The first is the inhibition of enzyme E by tryptophan. The second is the repression of transcription of mRNA, also tryptophan dependent. This genetic regulation is achieved through the activity of a repressor molecule R which, when bound to two units of tryptophan, interacts with an operator region of the operon, thus blocking transcription. The interactions are shown in Fig. 10.

The dynamics are as follows

$$\begin{aligned}
\frac{dM}{dt} &= K_m D \frac{O_t(P+K_d)}{P+K_d+\frac{R_t}{K_o}P} - (K_1+\mu)M \\
\frac{dE}{dt} &= K_e M - (K_2+\mu)E \\
\frac{dP}{dt} &= K_p E \frac{K_I^2}{K_I^2+P^2} - (K_3+\mu)P - 2k_2\frac{R_t P}{P+K_d} - (P_{\text{pro}}^m+\beta\mu)\mu C\frac{P}{P+K_s}.
\end{aligned}$$

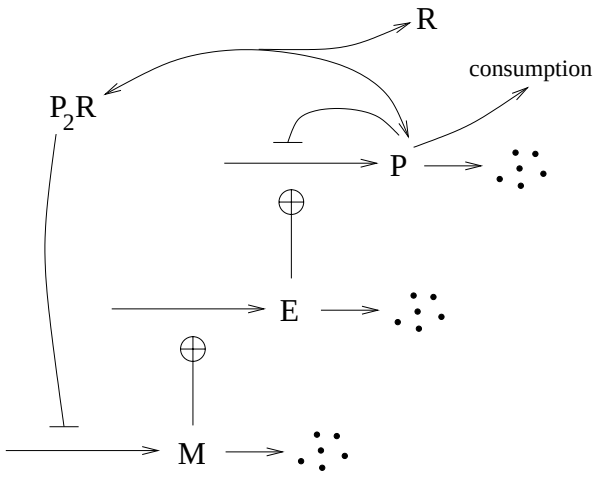

Fig. 10: Model of tryptophan biosynthesis

The parameters in the model are: the gene concentration D, the total operator concentration Q, the total repressor concentration R_t, the growth rate of the cells μ, the maximum protein concentration P^n_{pro}, the influence of growth rate on cellular protein concentration β, the molar percentage of tryptophan in cellular protein C, dissociation constants K_d, K_o and K_I, a saturation constant K_s, and rate constants K_m, K_e, K_p, K_1, K_2, K_3 and k_2.

Nondimensionalizing and taking appropriate parameter values (see [69]) leads to the equations

$$\begin{aligned}
\frac{dx(t)}{dt} &= \frac{z(t)+1}{1+(1+r)z(t)} - 0.909x(t) \\
\frac{dy(t)}{dt} &= x(t) - 0.0293y(t) \\
\frac{dz(t)}{dt} &= y(t)\frac{5210000}{5210000+z(t)^2} - 0.00936z(t) - 0.024\frac{z(t)}{z(t)+1} - \alpha_5\frac{0.00870z(t)}{z(t)+0.00500},
\end{aligned}$$

where x, y, and z are dimensionless concentrations of mRNA, enzyme, and tryptophan respectively. The behaviour of the system under changes in the value of α_5 will be addressed, with a nominal value of $\alpha_5 = 430$. The effect of the enzyme inhibition on this response will be illustrated by considering two values of the parameter r: strong feedback is exhibited with $r = 10$, while weaker feedback will be addressed by taking $r = 5$. The concentration of tryptophan (x) is taken as the output of the system.

The (magnitude) frequency responses to changes in α_5 are shown in Fig. 11. As discussed in [69], α_5 describes the effect of cellular demand for tryptophan. The behaviour shown in the Figure is typical of a negative feedback system. With weak feedback ($r = 5$), the effect of the input on asymptotic tryptophan levels decreases monotonically as the frequency grows larger. Strengthening the feedback (to $r = 10$) has two effects. The first is that the low frequency response is improved: as a standard sensitivity analysis would show, increasing the feedback reduces the effect of perturbations on the output. The other feature of stronger negative feedback is an increase in sensitivity at higher frequencies – to the point that the feedback actually makes the system *more* sensitive to disturbances over a certain frequency range.

The knowledge that negative feedback can introduce such resonance effects is crucial to the design of feedback systems. The tradeoff between improved response at low frequencies and increased sensitivity at higher frequencies can be made explicit (for certain linear systems) by a constraint known as

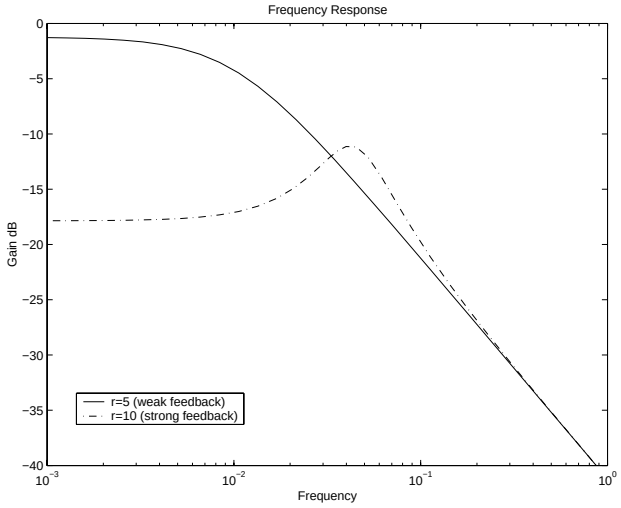

Fig. 11: Frequency response for *trp* operon model

Bode's Integral Formula [6]. System designers work around this "performance constraint" by implementing feedback which introduces increased sensitivity only at frequency ranges over which the system is unlikely to be excited. One could postulate that the same is true of feedback mechanisms within the cell: they have been crafted by natural selection in such a way that a trade-off is made between improved response to common low-frequency inputs and amplification of rare disturbances at higher frequencies. (Such an analysis has recently been applied to a model of glycolysis [16])

1.7.3 Regulation of Bacterial Chemotaxis: Integral Control

Lastly, a system employing integral feedback will be addressed. It was argued in [70] that the signal transduction network responsible for regulating bacterial chemotaxis achieves perfect adaptation through negative feedback involving an integral of the regulated variable. This powerful design is a regular feature in engineered feedback systems and no doubt is a common scheme in biochemical regulation. The analysis below is based on a model presented in [3]. A simplification of the model which retains the feedback structure has been derived [28] as shown in Fig. 12.

The model describes four states for the receptor complex R, which can be bound or unbound by ligand L, and methylated or demethylated. The reaction rates are given as

$$\begin{aligned} v_1 &= k_1[\mathrm{R}]\,[\mathrm{L}] - k_{1m}[\mathrm{RL}] \\ v_2 &= k_r([R]+[RL])[R] - k_b\, a_1^u[\mathrm{Rm}] \\ v_3 &= k_r([R]+[RL])[RL] - k_b\, a_1^o[\mathrm{RmL}] \\ v_4 &= k_1[\mathrm{Rm}]\,[\mathrm{RmL}] - k_{1m}[\mathrm{RmL}], \end{aligned}$$

where $k_r(\cdot)$ is a function which will be defined below. Nominal parameter values are chosen as

$$k_1 = 1000,\ \ k_{1m} = 1000,\ \ k_b = 1,\ \ a_1^u = 1,\ \ a_1^o = 0.25.$$

Initial conditions are chosen so that the total receptor complex concentration (which is invariant) is unity. The response to changes in the ligand concentrations will be considered, with a nominal value of

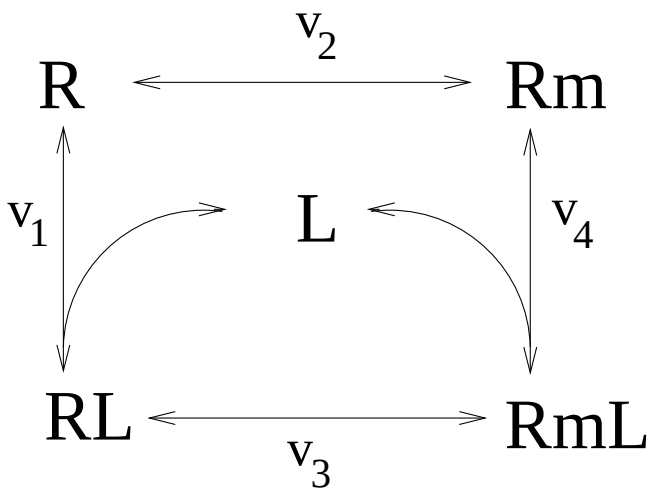

Fig. 12: Model of regulation of bacterial chemotaxis

[L]=1. The output of interest is the system activity level, which is taken as

$$A = a_1^u[\text{Rm}] + a_1^o[\text{RmL}].$$

Two choices for the function $k_r(\cdot)$ will be addressed. As described in [3] and [70] the system exhibits integral control action provided that the methylation reaction proceeds at saturation. This can be achieved by taking $k_r([\text{R}] + [\text{RL}]) = \frac{0.2}{[\text{R}] + [\text{RL}]}$. In this case a simple calculation shows that

$$\frac{d}{dt}([\text{Rm}] + [\text{RmL}]) = -A + 0.2,$$

so that the steady state value of A is clearly independent of [L]. The magnitude Bode plot showing the response in A to changes in [L] is shown in Fig. 13.

As expected, the response tends to zero at low frequencies and is zero at $\omega = 0$. The response reaches a maximum over a range of frequencies before dropping again at the system's bandwidth.

Alternatively, the methylation reaction could be chosen as non-saturated. This can be implemented by choosing linear dynamics with $k_r(\cdot) = 0.2$. This choice leads to the second frequency response shown in Fig. 13. The behaviour at higher frequencies is very similar to that described above. However, at low frequency a nonzero response is exhibited, indicative of negative feedback which does not employ integral action.

Other dynamics can be considered by alternative choices for the function $k_r(\cdot)$. By choosing saturable nonlinear dynamics (e.g. Michaelis-Menten type) one can explore the range between the frequency responses shown here. Such an analysis might capture the "true" nature of the chemotaxis control system. Although the system appears to exhibit an integral controller, there can be no doubt that the implementation is through a "leaky" integrator, and so the behaviour will be somewhere between the two extremes considered above.

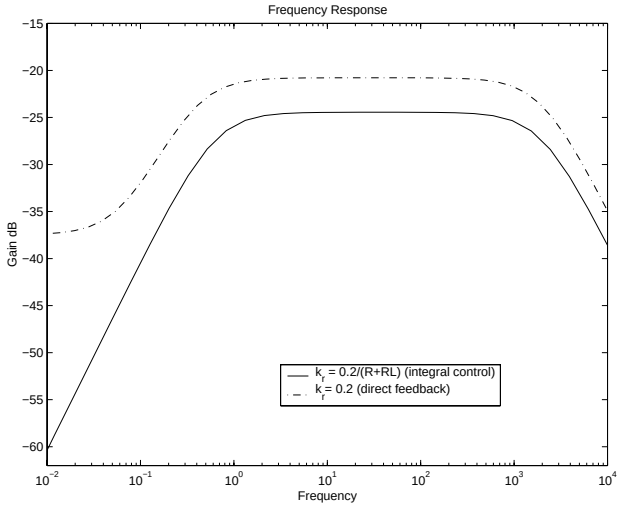

Fig. 13: Frequency response of chemotaxis model

2 Integral Feedback Control: From Homeostasis to Chemotaxis

2.1 Introduction

The goal of this section is to describe one particular type of feedback control, integral feedback, in which the output error is integrated and then fed back into the system. This type of control ensures robust perfect regulation: the steady-state error approaches zero in the presence of internal and external perturbations. Integral feedback is used ubiquitously in technological systems, and is likely to be a common control strategy in biological systems.

2.2 Primer on Integral Control

What is integral feedback control? It is a type of feedback structure that ensures the robust tracking of a specific steady-state value so that the error approaches 0 despite parameter variation. The term integral refers to the fact that the time integral of the system error is fed back into the system, not the error itself. Integral controllers are ubiquitious in man-made systems. For example, the cruise-control in a car uses integral control to maintain robustly the speed of the vehicle at the set point despite disturbances such as the wind or a hill.

A block diagram of a simple linear system with integral feedback illustrates its chief features (see Fig. 14). The plant or network, represented by the block with gain k, takes the input u and produces the output y_1. The difference between the output y_1 and the desired steady-state output y_0 is the error term y. Then, y is integrated and fed back into the system. The key to integral control is that the feedback term $x = \int y$ so that

$$\dot{x} = y.$$

At steady-state the time derivatives of the variables go to 0, so that $y \to 0$ as $t \to \infty$ independent of the values of the input u and the gain k. Hence, the error asymptotically approaches 0 as long as the system is stable.

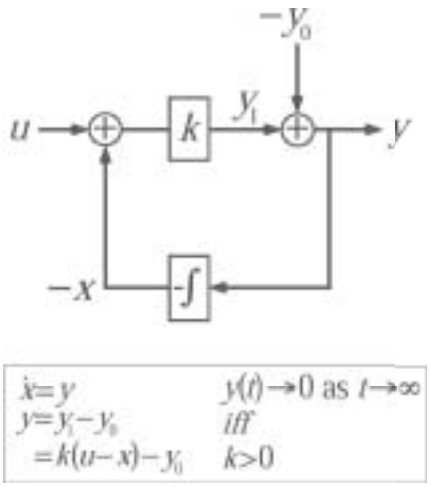

Fig. 14: A block diagram of integral feedback control. The input is u, the gain is k, y is the net deviation from the steady-state output y_0, x is the feedback term.

2.2.1 Types of feedback control

There are three basic types of feedback control: (1) proportional control, the error term is multiplied by a constant before being fed back; (2) integral control, error is integrated as described above; or (3) derivative control, error is differentiated (see Fig. 15). Each type of feedback has beneficial features. Proportional control corrects for "current" errors. One can adjust the amount of feedback by increasing or decreasing the constant factor. Higher feedback gain is better at rejecting disturbances, but it also causes the system to become less stable. As described above, integral control eliminates steady-state errors. Finally, derivative control provides "anticipation" of upcoming changes, which increases damping, improves stability, and decreases transient errors.

To capture the best properties of all three controllers, one can combine them into a proportional-integral-derivative (PID) control system. The transfer function for a PID controller is written as $PID(s) = K(1+\frac{1}{T_I s}+T_D s)$. One can obtain the desired performance by tuning the parameters K, T_I, and T_D to get the best balance of steady-state error, transient behavior, and stability. It is helpful to think about more complex controllers in these simple terms in order to gain intuition.

2.2.2 Transfer Function Interpretation

One can transform (Laplace) a time domain representation of a linear system into a frequency domain description composed of transfer functions. Given a typical linear feedback system with plant P and controller C, the sensitivity transfer function from a disturbance input to the output is $S(s) = \frac{P(s)}{1+P(s)C(s)}$ (see Fig. 15). We can then prove that if the input signal is a step of size k ($U(s) = k/s$), then $y(t) \to 0$ as $t \to \infty$ iff S(s) has a zero at the origin [15].

In transfer function form, $Y(s) = U(s)S(s) = \frac{kS(s)}{s}$. If the feedback system is stable, then by the final value theorem $y(t) \to kS(0)$ as $t \to \infty$. Clearly, the right-hand side is zero iff $S(0) = 0$. An integral feedback system possesses such a zero at the origin: $S(s) = \frac{sP(s)}{s+P(s)}$.

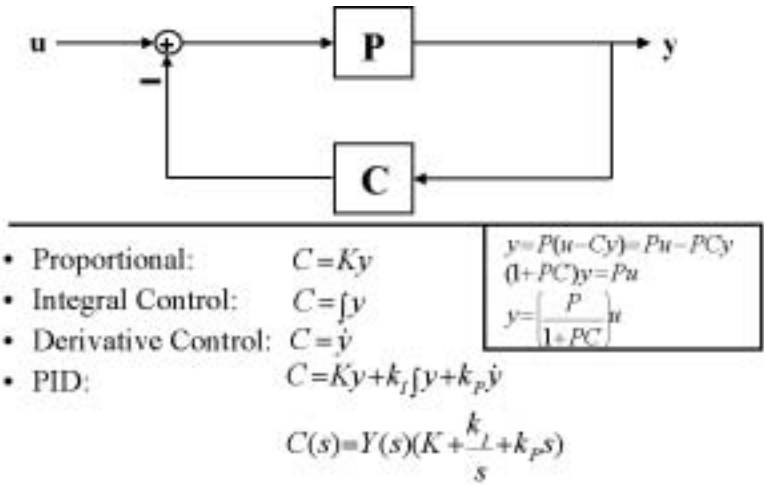

Fig. 15: Basic types of feedback control. The block P represents the plant (e.g., signaling pathway), and C represents the feedback control block. Proportional, integral, derivative and PID controllers are defined. The transfer function from the input U to the output Y is calculated.

2.2.3 State-Space Interpretation

One can represent the dynamics of a system in state-space form as a set of first order differential equations: $\dot{x} = f(x,u)$, $y = g(x,u)$. The vector x is the state of the system (e.g., concentrations of the species), and u is the input. For a linear system, we can simplify this description to the following matrix form:

$$\begin{aligned} \dot{x} &= Ax + Bu \\ y &= Cx + Du \end{aligned}$$

One can introduce a new integral feedback state z with the dynamics $\dot{z} = Cx + Du = y$. Clearly, these dynamics are sufficient to ensure that the steady-state error approaches zero. What about necessity? One can demonstrate that integral control is necessary for robust perfect regulation in the following manner.

At steady-state $\dot{x} = 0$, so that $x = -A^{-1}Bu$ and $y = (D - CA^{-1}B)u$. Thus, y = 0 at steady-state for all constant u, iff either

$$[\ C \quad D\ ] = 0 \text{ or } \det \begin{vmatrix} A & B \\ C & D \end{vmatrix} = 0$$

The former is the trivial case when $y(t) = 0$ for all t, and the latter holds iff $\exists k \neq 0$ such that $k[\ A \quad B\ ] = [\ C \quad D\ ]$. Thus, defining $z = kx$, we have $\dot{z} = kx = k(Ax + Bu) = Cx + Du = y$, which is the standard integral control equation.

2.3 Examples of Integral Control in Biology

2.3.1 Bacterial Chemotaxis Signaling Pathway

Bacteria are able to sense gradients of attractants and repellents. The signal transduction pathway responsible for this behavior possesses several special features to ensure both exquisite sensitivity and wide dynamic range. One such feature is perfect adaptation: the output of the pathway (flagellar rotation) exactly returns to its prestimulus value even in the presence of continual stimulation so that the steady-state level of output activity asymptotically approaches a constant value independent of the attractant concentration.

The bacterial chemotaxis system is a two-component signaling system [64]. The receptor complex, which consists of the receptor, the histidine kinase CheA, and the adaptor protein CheW, phosphorylates the response regulator CheY. Phosphorylated CheY interacts with the flagellar motor to induce clockwise (CW) rotation and tumbling behavior. Attractant inhibits the receptor complex resulting in counterclockwise (CCW) flagellar rotation and straight runs. Receptor complex activity is regulated by methylation which mediates adaptation. Methylation by CheR increases receptor activity; demethylation by CheB decreases activity. Although there is no direct evidence, we assume that CheB senses the activity state of the receptor by only demethylating active receptor complexes. This assumption results in an important negative feedback loop.

Model of bacterial chemotaxis signaling There are many models of this system [61, 7, 23, 63]. We have focused on a simplified version of the Barkai-Alon-Leibler model (BAL) [3]. The receptors in this basic model possess two methyl groups instead of the usual four methyl groups. The focal point of this model is the receptor complex, denoted E, which consists of Receptor + CheA + CheW. This complex possesses two states: active and inactive. When active, E phosphorylates the response regulator protein CheY to form CheY-P. System activity refers to the concentration of active receptor complexes.

The receptor complex can bind ligand and is modified by methylation on two sites ($m = 0, 1, 2$). The ligand occupied and unoccupied forms are denoted E_m^o and E_m^u, respectively. CheR methylates the receptor complex and CheB demethylates the receptor complex. The probability that a given species of E is active depends on the methylation level and ligand occupancy of the receptor and is denoted α_m^i ($i \in \{o, u\}$). A typical equation is as follows consisting of ligand binding, methylation and demethylation terms:

$$\frac{dE_0^o}{dt} = (k_l l E_0^u - k_{-l} E_0^o) - (V_{mth} E0o) + (V_{dmth}[E1o \cdot a1o])$$

A more complete listing of the model can be obtained from the SBML file for this model (ICSB2002_Chemotaxis.sbml).

2.3.2 Robust versus non-robust perfect adaptation

Experimental results Alon, Leibler and colleagues tested the robustness of perfect adaptation to dramatic changes in the concentration of key components of this pathway [2]. They demonstrated that as the methylase CheR was varied over a 50-fold range, the adaptation precision remained close to perfect. They went on to show that perfect adaptation was robust not only to changes in levels of CheR, but also to changes in the concentration of CheB, receptor, and CheY.

Theoretical results Is it possible to model perfect adaptation in bacterial chemotaxis? Most models in the literature indeed are able to reproduce perfect adaptation, but only through fine-tuning of the model parameters. Perfect adaptation is non-robust in these models because altering a parameter disrupts perfect adaptation. Alternatively, one can imagine that perfect adaptation is a structural property of the system, insensitive to parameter variation, perhaps resulting from a particular feedback control mechanism. To distinguish between these two types of models, we have systematically varied model parameters and tested for perfect adaptation using continuation methods.

In Model A, the parameter that was varied was the total receptor concentration over a 100-fold range (see Fig. 16A). On the y-axis we plotted the steady-state output for three concentrations of ligand as we varied the total receptor concentration. As one can see, perfect adaptation was achieved for only one value of receptor concentration, 8 mM.

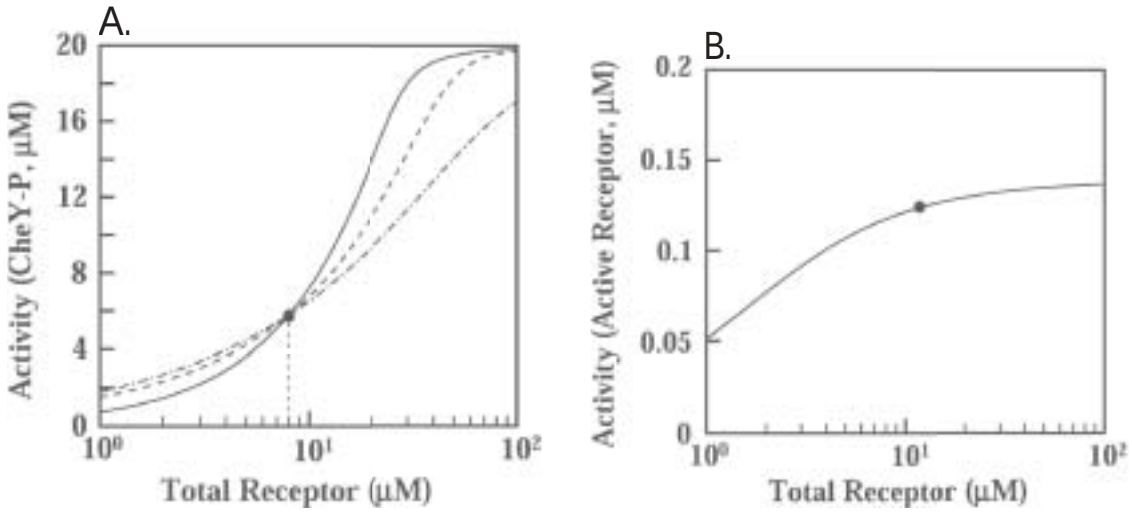

Fig. 16: Robust and nonrobust perfect adaptation. The dependence of steady-state system activity on total receptor concentration was calculated by using equilibrium analysis for three concentrations of chemoattractant: (i) $L = 0$ (solid), (ii) $L = 1$ μM (dashed), and (iii) $L = 1$ mM (dashed dot). The filled circle indicates the value of total receptor used in the model. **A.** Model A, perfect adaptation exists only at a single value of total receptor. **B.** Barkai-Alon-Leibler model, perfect adaptation holds for a range of total receptor concentration.

In the BAL model, the steady-state receptor at the 3 concentrations of attractant completely superimposed as one varied the total receptor concentration (see Fig. 16B). Perfect adaptation was robust to a 100-fold change in receptor concentration.

Bifurcation diagram One is often interested in studying the dynamics of a system as a function of a specific parameter (e.g., total receptor concentration). In some cases, the dynamics change quantitatively – the steady-state value of the output in Fig. 16 increased as total receptor increased. In other cases, the dynamics may change qualitatively with the steady-state disappearing or becoming unstable, or with new steady-states being created. These qualitative changes in dynamics are termed bifurcations, and are best depicted in bifurcation diagrams [66]. Programs such as AUTO [14] can be used to generate bifurcation diagrams from a differential equation model.

Implementation of integral control in chemotaxis system How is integral control implemented in the BAL model of the chemotaxis system? A simplified version of the derivation is shown here. The variable x represents the methylation state of the receptor. The change in x, $\dot{x}$, equals the methylation rate r minus the demethylation rate. Using the assumption that CheB only demethylates active receptor complexes so that the demethylation rate is a linear function of A, we obtain the following: $\dot{x} = r - bA$. At steady-state, $\dot{x} = 0$, $r = bA$, and hence the steady-state activity level $A^0 = r/b$. We can rewrite this as the familiar $\dot{x} = -b(A - A^0) = -by$. The key point is that if r and b are independent of u, then this system will exhibit perfect adaptation that is robust to changes in the system parameters.

2.3.3 Blood Calcium Regulation

The level of calcium in the blood is carefully regulated against disturbances in calcium utilization and uptake. The two compounds parathyroid hormone (PTH) and vitamin D (VitD) play a central role in

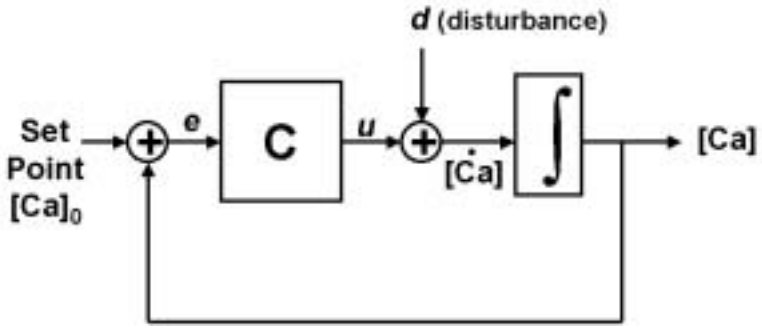

Fig. 17: Model of blood calcium regulation [17]. A disturbance d in calcium dynamics is attenuated by the control action u mediated by PTH and vitamin D, which are represented by the block C. The error e is the current level of calcium, [Ca], minus the set point level of calcium, $[\mathrm{Ca}]_0$.

this regulation. They control how much calcium is introduced into the blood from the intestine (vitamin D) and from the bone (PTH). El-Samad and Khammash have formulated the following model [17] of these dynamics in mammals. The model is illustrated schematically in Fig. 17.

A disturbance d affects the rate at which calcium is taken up or removed from the blood; this disturbance is compensated for by the action of PTH and vitamin D, u: $d[\mathrm{Ca}]/dt = u + d$. The error is the deviation from the steady-state blood calcium level ($e = [\mathrm{Ca}] - [\mathrm{Ca}]_0$). It is known from physiological measurements that the level of PTH is proportional to this error ($e \propto [\mathrm{PTH}]$). In addition, the rate of production of vitamin D is proportional to the concentration of PTH, and assuming that vitamin D has a slow degradation rate on the time scales of interest, we have $d[\mathrm{VitD}]/dt = k[\mathrm{PTH}]$. Thus, we can calculate the error in terms of [PTH] or [VitD]: $e = k_1[\mathrm{PTH}] = k_2 \dot{d}[\mathrm{VitD}]/dt$. Finally, if we approximate the rate of calcium absorption from the intestine or bone as linear functions of [VitD] and [PTH], respectively, we have the following equation for the control action: $u = k_3[\mathrm{PTH}] + k_4[\mathrm{VitD}] = k_p e + k_i \int e$. Thus, this system exhibits proportional-integral (PI) control.

2.4 Integral control, the Internal Model Principle, and homeostasis

2.4.1 Homeostasis

Homeostasis is the dynamic self-regulation of a system to maintain essential variables within limits necessary for acceptable performance in the presence of unexpected disturbances. Homeostasis is one of the defining features of living organisms. A related concept is that of adaptation in which the system adjusts itself to be better suited to new environmental conditions. In signal transduction, adaptation refers to the process in which the output returns toward its prestimulus value in the presence of a continuous stimulus. Adaptation is important for maintaining sensitivity and dynamic range in sensory systems.

2.4.2 Necessity of integral control

An important point is that integral feedback control is not only sufficient, but also necessary for robust perfect adaptation. Thus, even if the BAL model is invalidated by future experiments, another mechanism implementing integral control must be present in the bacterial chemotaxis signaling pathway to explain the robust perfect adaptation. More generally, biological systems that require that calcium or some other internal variable maintain a constant steady-state value despite step changes in some input must have integral feedback as a structural feature of the network. A simple proof of the necessity

of integral control for linear systems was provided in the previous section. A more general proof for nonlinear systems is outlined in the references described below.

This necessity statement suggests that integral control is prevalent at all levels of biology from cellular regulation, to organismal physiology to ecosystem balance. In complex man-made systems, integral control loops are found at every level from CPUs to instruments to the entire vehicle. A single oil refinery possesses more than 10,000 integral feedback loops.

2.4.3 Internal model principle

The internal model principle (IMP) is a generalization of the necessity of integral control. The principle states that the robust tracking of an arbitrary signal requires a model of that signal to be in the controller. The intuition is that the internal model counteracts the external signal so that $y(t) \rightarrow 0$ as $t \rightarrow \infty$ even in the presence of parameter perturbations. For example, a controller containing an integrator is necessary to track robustly a step signal, which is the impulse response of an integrator.

Francis and Wonhams proved IMP for linear systems [20]. Isidori and colleagues have established a general framework for IMP in nonlinear systems [34]. Sontag has provided a succinct statement of IMP relevant to biological systems. We will sketch the ideas behind these proofs in the tutorial.

It is important to appreciate that living systems are subject not only to constant changes (steps). but also to perturbations that involve steadily rising or falling signals (ramps), and to even more complex disturbance behaviors (e.g., neural signals). In order to maintain homeostasis, the feedback control system implemented by the biological network must contain an internal model of the disturbance according to IMP. An area for future research is cataloging these control structures and addressing the question of how biology builds these internal models.

2.5 Integral Feedback and Chemotaxis

2.5.1 Temporal and Spatial Sensing of Gradients

Given a spatial gradient of some attractant, $C(x,t)$, there are two basic chemotactic strategies: temporal sensing and spatial sensing. In temporal sensing, the organism measures C at two different time points, t_1 and t_2. If $\frac{(C(t_2)-C(t_1))}{(t2-t1)} = \frac{dC}{dt} > 0$, then the organism must be going up the gradient, and it continues to move in the same direction. If $\frac{dC}{dt} < 0$, the organism must be moving down the gradient, and so it reorients itself.

In spatial sensing, the organism measures C at two different locations, x_1 and x_2. If $\frac{(C(x_2)-C(x_1))}{(x2-x1)} = \frac{dC}{dx} > 0$, then the organism moves in the direction of x_2; otherwise, it moves in the direction of x_1. Clearly temporal sensing is suited for smaller motile organisms, whereas spatial sensing is preferable for larger stationary organisms.

2.5.2 Estimating dC/dt Using Integral Feedback

An organism chemotaxing up an attractant gradient wants to maximize dC/dt. For temporal sensing, this entails an accurate calculation of dC/dt, i.e., implementing a differentiator. The simplest arrangement is to insert a differentiator into the forward signaling pathway from attractant receptor to effector (i.e., flagella) so that $Y(s) = sP(s)U(s)$, where $U(s)$ is the input, $sP(s)$ is the transfer function for the signal transduction cascade, and $Y(s)$ is the output. It should be noted that $sU(s)$ is the Laplace transform of du/dt. Alternatively, one can construct the differentiator by placing an integrator into the feedback

loop regulating the signaling pathway, i.e. integral control, so that $Y(s) = \frac{sP(s)U(s)}{P(s)+s}$. There are two advantages to integral control: (1) noise reduction – an open-loop differentiator will amplify high-frequency variations in the input signal, (2) robustness – variations in the plant could disrupt the differentiator.

While this model explains well the high frequency behavior of the network regulating chemotaxis [2], other system-theoretic aspects have not been considered. Bacteria live in very noisy environments [5], however, and so differentiation must be coupled with a low-pass filtering mechanism. In particular, after tumbling, cells must be able to discern their new alignment with the external chemoattractant gradient while being subjected to high thermal noise. A simple model of this can be obtained for this system and the optimal filter derived. The predicted optimal filter is a low-pass filter with a bandwidth of approximately 0.3 rad/s (unpublished notes) which agrees closely with published models of the chemotactic network [63].

In fact, having a integrator in the feedback loop accomplishes the dual goals of infinitely high gain at low frequencies (integral control) and low gain at high frequencies (low-pass filtering) which seems to be an optimal chemotactic strategy for systems that rely on temporal gradient sensing.

In the next section we consider a eukaryotic system's chemotactic mechanism and demonstrate how it relies on both negative *and* positive feedback.

3 Cellular communication: Uses of positive and negative feedback

In the previous sections we saw how integral control can be used to achieve robust perfect regulation. Here we parallel the roles played by feedback control systems in engineering applications with those present in some cell signaling pathways. We concentrate on the pathway associated with *chemotaxis* — directed cell locomotion — in the social amoeba *Dictyostelium discoideum* [36]. For recent reviews of the chemotactic signaling pathways involved in *Dictyostelium* in the biology literature, see [9, 32, 51].

Gradient sensing and chemotaxis in *Dictyostelium discoideum*

Dictyostelium are social amoebae (also known as slime molds) that live in the soil as separate, independent cells, feeding on bacteria. When facing adverse environmental conditions, such as when all the bacteria are consumed and starvation is imminent, they begin to interact to form multicellular structures. This developmental process is illustrated in Fig. 18.

Approximately 6 hours after commencing development, up to 100,000 cells will signal each other by synthesizing and releasing the chemoattractant cyclic-AMP (cAMP). Cells are able to detect pulses of cAMP and use spatial differences in the concentration of cAMP to move towards each other and aggregate. The ability to sense the direction of external chemical sources and respond by polarizing and migrating toward chemoattractants or away from chemorepellants — a process known as chemotaxis — is crucial for the survival of *Dictyostelium*. Many of the mechanisms employed by *Dictyostelium* to chemotax — including the sensing of the chemotactic molecule, the activation of the signal transduction pathway and the cell mobilization — are shared with other organisms, including mammalian cells.

3.1 Feedback: balance between robustness and gain

3.1.1 Negative feedback

As pointed out previously, one of the reasons for employing a negative feedback regulator to achieve perfect adaptation is that this is a very robust architecture. This has been known in an engineering setting since 1927 when Harold Black received a patent for the use of negative feedback in amplifiers [4]. As

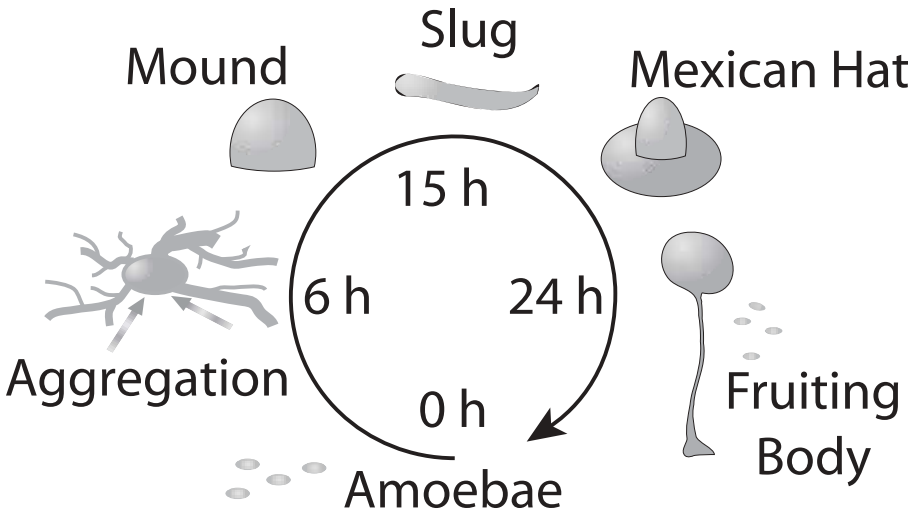

Fig. 18: ***Dictyostelium* life cycle.** *Dictyostelium* usually live as single cell amoebae. However, when faced with adverse environmental conditions, they commence a developmental change. Approximately six hours after this trigger, cells use *chemotaxis*, chemically-guided locomotion, to aggregate. Eventually, up to 10^5 cells can come together. The multicellular organism undergoes a series of morphological changes that eventually lead to a resistant spore suspended on a stalk (24 h).

explained in Fig. 19, the use of negative feedback in a closed-loop system will decrease the overall system's sensitivity to parameter variations. While this is widely understood by control engineers, it is really only now beginning to be noticed by biologists. In bacterial chemotaxis, which is also regulated via an integral feedback control mechanism, there is now experimental evidence for this robustness. Alon and co-workers, by varying the expression levels of some of the proteins regulating chemotaxis [2] found that the adaptation property was maintained even when some of these levels changed up to 50 times; see [70] for a discussion. In *Dictyostelium* chemotaxis, there has been no systematic experimental test of whether the adaptation mechanism is robust.

In addition to providing increased robustness to the system, negative feedback allows systems that are open-loop unstable, to be stabilized. The earlies uses of such systems in engineering are the flywheel governors used in the 18th century to control steam engines.

3.1.2 Negative feedback in *Dictyostelium* chemotaxis.

The basic mechanism regulating chemotaxis in *Dictyostelium* is shown in Fig. 20. Binding of the extracellular cAMP to the cAMP-receptors (CAR1) leads to the activation of several "downstream" processes. CAR1 is coupled to a heterotrimeric G-protein; upon stimulation, the α subunit dissociates from the β and γ subunits. The latter two subunits are known to activate a series of events involving a cascade of phosphoinositides. [10] These lipids can be phosphorylated and dephosphorylated at a series of sites. The key event in the chemotaxis response seems to be the phosphorylation of the lipid PIP_2 (phosphatidylinositol 4,5-bisphosphate) by the kinase PI3K (phosphoinositide-3-kinase) to form PIP_3 (phosphatidylinositol 3,4,5-trisphosphate) and its dephosphorylation by the phosphatase PTEN (phosphatase and tensin homolog).

In addition to playing opposite roles in the conversion of PIP_2 to PIP_3, the two enzymes PTEN and PI3K also have complementary behavior. PTEN is initially bound to the inner leaf of the membrane

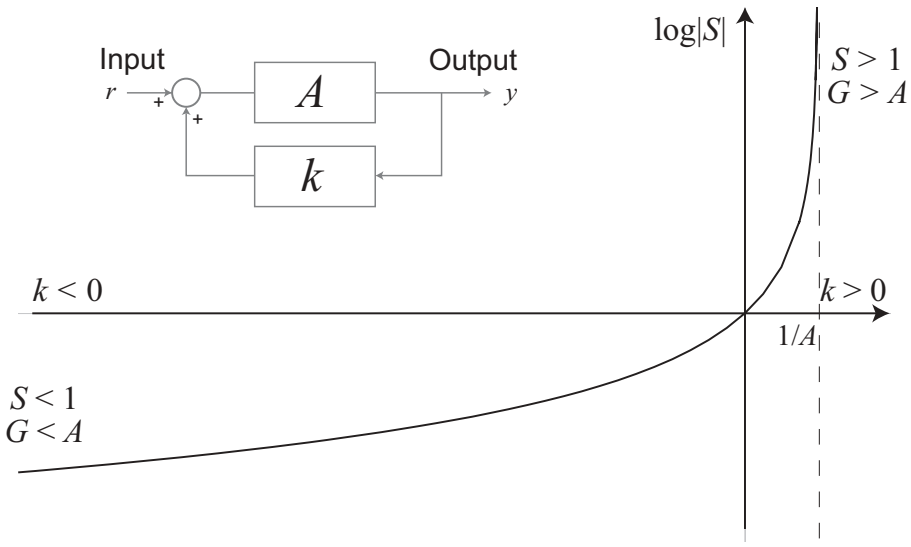

Fig. 19: **Sensitivity/gain tradeoffs in feedback control.** For a constant gain amplifier A with feedback gain k, this figure shows the tradeoff between small sensitivity and high amplification. The gain of the system is defined as the ratio of output y over input r and is given by $G = A/(1-kA)$. The sensitivity is $S = (\partial G/\partial A)/(G/A) = 1/(1-kA)$. In particular, negative feedback ($k < 0$) provides low sensitivity ($S < 1$) at the cost of low gain ($G < A$). In *Dictyostelium* chemotaxis, this is used to "filter out" the mean level of external signal. This allows the cell to chemotax at both high and low signal levels. Positive feedback ($k > 0$) is used to amplify signals. In *Dictyostelium* this is used to increase the sensitivity to spatial gradients of chemoattractant, thereby allowing the cell to chemotax to far away sources.

and is released into the cytosol upon stimulation. Simultaneously, PI3K , which is initially in the cytosol, translocates to the cell membrane. The appearance of PIP_3 creates a binding site that permits the relocalization of CRAC (cytosolic regulator of adenylyl cyclase) to the plasma membrane.

When stimulated by a constant and persistent cAMP signal, the events that are downstream from the G-protein exhibit adaptation. As with bacterial chemotaxis, adaptation here serves to filter out spatially homogeneous steady-state levels of cAMP. By allowing the cell to focus on the differences in concentration of cAMP, the cell is able to detect gradients both far and near to a cAMP source.

A mathematical model. Here we describe a possible model for the adaptation mechanism found in *Dictyostelium*. We begin by postulating the existence of a *response regulator* that can exist in one of two confirmations: active and inactive. Denote by $R^\star$ (resp. R) the concentration of an active (resp. inactive) components and assume that the total number is constant, so that: $R_{\mathrm{T}} = R^\star(t) + R(t)$.

One can think of the active and inactive forms of the regulator as representing the binding sites for PI3K and PTEN respectively that exist on the cell membrane.

We assume that the activation and inactivation are regulated by a pair of enzymes: A, and I respectively. Using mass action dynamics, an equation for the system is

$$\begin{aligned}\frac{dR^\star(t)}{dt} &= -k_{-r}I(t)R^\star(t) + k_r A(t)R(t) \\ &= -\big(k_{-r}I(t) + k_r A(t)\big)R^\star(t) + k_r A(t)R_{\mathrm{T}} \end{aligned} \tag{16}$$

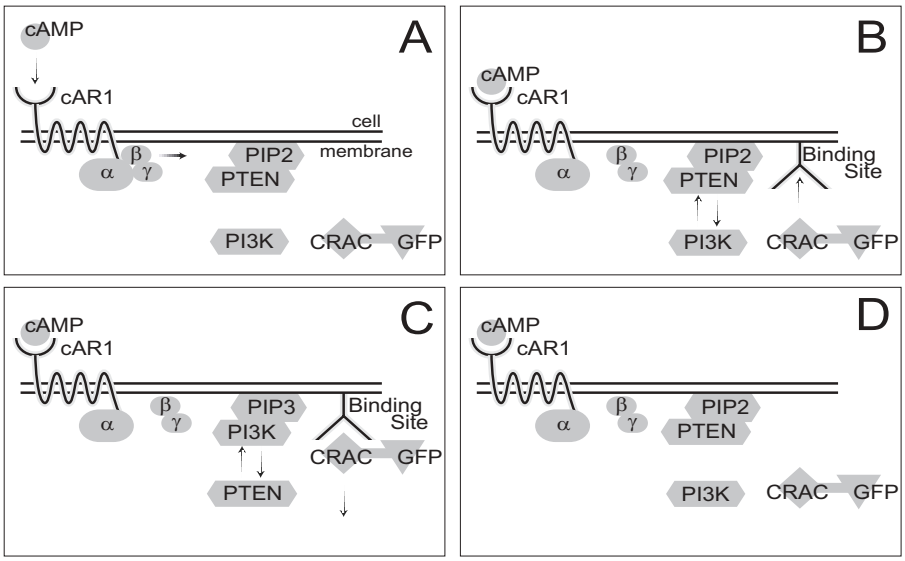

Fig. 20: **Chemoattractant response.** A. Before stimulation by extracellular cAMP, the cAMP receptor (CAR1) is coupled to the heterotrimeric G-protein that consists of α, β and γ subunits. The lipid PIP_2 and lipid phosphatase PTEN are found on the membrane whereas the kinase PI3K and CRAC are in the cytosol. The latter can be fused with a green fluorescent protein (GFP) so that its translocation can be monitored using fluorescent microscopy. This serves as a readout of the cell's response. B. Upon binding to the receptor, the G-protein α subunit dissociates from the $\beta\gamma$ subunits. This triggers a release of PTEN and a recruitment of PI3K to the inner leaf of the plasma membrane. C. PI3K phosphorylates PIP_2 creating PIP_3. This creates a binding site for CRAC-GFP. D. After an initial transient, the cell adapts to this stimulus. In particular, despite the fact that the ligand cAMP is still bound to the receptor, and that the G-protein is still dissociated, the CRAC is observed to return to its exact prestimulus level. PIP_2, PIP_3, PTEN and PI3K levels also return to prestimulus levels, though not perfectly in some cases. The peak levels of activity, measured by membrane-bound CRAC occur approximately 5 seconds after stimulation; by 20 seconds, most of the cell has adapted.

The steady-state fraction of active regulators is

$$\lim_{t\to\infty}\frac{R^\star(t)}{R_{\rm T}}=\frac{A(\infty)/I(\infty)}{K_R+A(\infty)/I(\infty)} \tag{17}$$

where $K_R=k_{-r}/k_r$. Note that it is the *ratio* of enzyme concentrations that determines the steady-state concentration of active receptors. Now, assume that these enzymes are, in turn, regulated by the external signal S which is proportional to chemoattractant concentration:

$$\frac{dA(t)}{dt}=-k_{-a}A(t)+k_aS(t) \tag{18}$$

$$\frac{dI(t)}{dt}=-k_{-i}I(t)+k_iS(t) \tag{19}$$

Suppose that the cell is initially at steady-state with cAMP concentration $S_0\neq 0$ and that, at time $t=0$, this is changed to $S_1\neq 0$. The enzyme concentrations obey

$$A(t)=A_1+e^{-k_{-a}t}(A_0-A_1)$$

$$I(t)=I_1+e^{-k_{-i}t}(I_0-I_1)$$

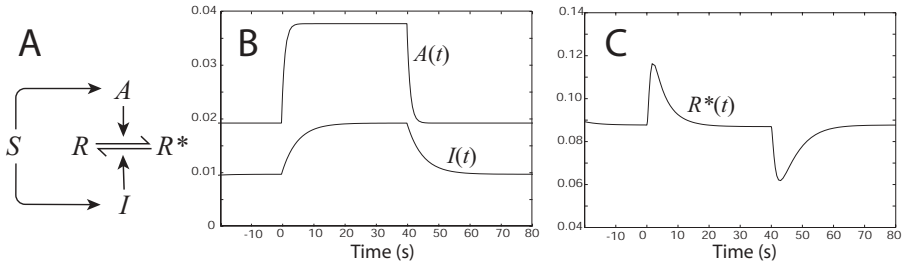

Fig. 21: **Activator/inhibitor model of adaptation.** A. In this model, a response regulator can be found in either an active, $R^\star$, or inactive, R, form. Changes between the two states are mediated by either the activator A or inactivator I. These both respond to the external signal S. B. A change in the signal S at 0 s causes a rapid increase in the concentration of $A(t)$ followed by a slower increase in that of $I(t)$. By about 20 s, both have reached steady-state values. The external signal level is decreased at 40 s causing the opposite responses. C. The active response regulator output. During the time when $A(t)$ but not $I(t)$ has reached its new equilibrium, there are transient changes in the concentration of $R^\star(t)$. These subside as $I(t)$ "catches up" to $A(t)$.

where $A_j = S_j K_A$, $I_j = S_j K_I$, for $j = 0, 1$ and $K_A = k_a/k_{-a}$, $K_I = k_i/k_{-i}$.

These expressions can then be replaced in (17) to show that the steady-state concentration of active response regulators is independent of cAMP concentration. It follows that the system is rejecting the step changes in cAMP perfectly.

Taking bacterial chemotaxis as a model, we would expect that a system that is rejecting step disturbances as this one is would have an integrator in the feedback path. To show that this is the case, we rewrite the differential equation for $R^\star$ as

$$\frac{dR^\star(t)}{dt} = -\big(k_{-r} I(t) + k_r A(t)\big)\big(R^\star(t) - S^\star(t)\big) \tag{20}$$

where

$$S^\star(t) = R_{\mathrm{T}} \frac{A(t)/I(t)}{K_R + A(t)/I(t)}$$

Moreover,

$$\begin{aligned} \frac{A(t)}{I(t)} &= \frac{A_1}{I_1} \frac{1 + e^{-k_{-a}t}(A_0/A_1 - 1)}{1 + e^{-k_{-i}t}(I_0/I_1 - 1)} \\ &= \frac{A_1}{I_1} + \text{“transient”} \\ &= \frac{K_A}{K_I} + \text{“transient”} \end{aligned}$$

Thus, $S^\star(t)$ acts as an external disturbance consisting of a decaying transient and a persistent, constant signal whose value depends only on kinetic parameters.

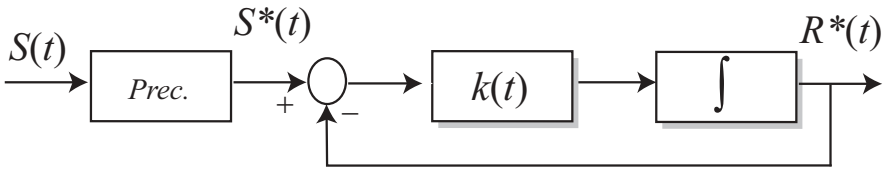

Fig. 22: **Integral feedback.** Using the form of (20), the adaptation mechanism of *Dictyostelium* can be seen to possess an integral feedback form with a precompensator. The signal $S^*(t)$ includes a persistent component K_A/K_I and a decaying part.

The feedback system can now be redrawn as in Fig. 22. We see from the differential equations for $A(t)$ and $I(t)$ that these enzymes act as a feedforward system specifying the constant reference signal. The system of Fig. 21 then acts as an integral control feedback with time-varying gain given by $k(t) = k_{-r}I(t) + k_rA(t)$. Because of the form of (16), the closed-loop system is asymptotically stable provided there exists an $\varepsilon > 0$, such that $k(t) > \varepsilon$ for all time. This is guaranteed provided that the external signal $S(t) > \delta$ for all t and some $\delta > 0$.

Note that to generate step increases in response to the chemotactic source we require that the transient increase in $A(t)$ be larger than that of $I(t)$. If this is the case, $S^*(t)$ will also increase transiently causing an increase in the concentration of $R^*(t)$. This is guaranteed, provided that $k_{-a} > k_{-i}$.

If we reverse this inequality, then an increase in chemoattractant concentration would result in a *decrease* in the number of active response regulators. This does not seem to play a part in *Dictyostelium* chemotaxis, but may be of significance in other systems. For example, in the chemotactic response of nerve growth cones, it is known that the same chemical may act either as an attractant or repellant [47]. Our model could account for this by modulating either of the kinetic parameters k_{-a} or k_{-r} so as to ensure that $S(t)$ causes increases or decreases in R^*, thereby turning chemical attraction into repulsion.

3.2 Engineering uses of positive feedback

As described in Fig. 19, positive feedback can give rise to an increase in the sensitivity of a linear system. This was actually understood in engineering a full fifteen years before Black's discovery [4]. If positive feedback: $k > 0$ is chosen, the system gain will increase significantly, at the cost of increased sensitivity to noise and other disturbances.

This engineering insight has led several groups to suggest mechanisms providing gradient amplification based on positive feedback loops [30, 43, 46, 50, 52, 53].

3.2.1 Amplification and positive feedback

One drawback of the model presented above to describe *Dictyostelium* chemotaxis is that the resultant spatial response for the binding sites is, at best, that of the external chemoattractant gradient. That is, a 10% difference in chemoattractant concentration between front and back can only give rise to an equal 10% difference in response. Experimental evidence is for greater differences in the response than in the stimulus [51].

A possible model for amplification using positive feedback. In Fig. 23 a putative positive feedback mechanism is outlined. Let p_1, p_2 and p_3 represent the relative concentrations of PIP, PIP_2 and PIP_3,

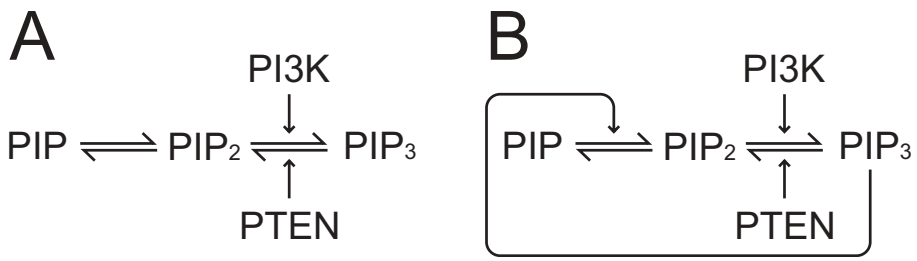

Fig. 23: **Possible positive feedback configurations.** A. This model shows the signaling cascade involving the different phosphoinositides. PIP, PIP_2 and PIP_3 are phosphorylated once, twice or three times respectively. Phosphorylation of PIP_2 is mediated by the kinase PI3K whereas dephosphorylation by the phosphatase PTEN. B. In this scheme, a positive feedback loop is postulate from PIP_3 to the production of PIP_2.

with $p_1 + p_2 + p_3 = 1$ [29]. As a baseline, we point out that, if there is no feedback mechanism, the concentrations of the lipids follow:

$$\frac{dp_1(t)}{dt} = -k_1 p_1(t) + k_{-1} p_2(t) \tag{21}$$

$$\frac{dp_3(t)}{dt} = -k_{-2} v(t) p_3(t) + k_2 u(t) p_2(t) \tag{22}$$

where $u(t)$ and $v(t)$ are the concentrations of PI3K and PTEN respectively. Solving for steady-state, we arrive at:

$$p_2 = \frac{v}{v(1+\alpha) + u\alpha\beta}, \qquad p_3 = \frac{u\alpha\beta}{v(1+\alpha) + u\alpha\beta}$$

where $\alpha = k_1/k_{-1}$ and $\beta = k_2/k_{-2}$.

We now consider the positive feedback model of Fig. 23B. There is evidence in some organisms other than *Dictyostelium* that also use the PIP_2/PIP_3 pathway for signaling that there is a positive feedback loop from PIP_3 to at least one of the precursors, such as PIP [11]. We can account for this feedback by modifying (21) according to:

$$\frac{dp_1(t)}{dt} = -k_1\big(\varepsilon + p_3(t)\big) p_1(t) + k_{-1} p_2(t)$$

Rather than solving this for the general case, we will assume that the feedback gain is large enough so that

$$\frac{dp_1(t)}{dt} \approx -k_1 p_3(t) p_1(t) + k_{-1} p_2(t)$$

We can now solve for the steady-state of the system. We find that the system undergoes a transcritical bifurcation depending on the parameter $\gamma = u/v$. For small values of u/v, the only stable steady-state is p_3=0. The threshold occurs when

$$\gamma_{\text{th}} = \frac{1}{\alpha\beta}$$

at which point

$$p_3 = \frac{\gamma - \gamma_{\text{th}}}{\gamma + 1/\beta}$$

This configuration could explain the amplified nonlinear response seen in gradient sensing in *Dictyostelium*. In particular, the response regulator described in Section 3 could serve to regulate PI3K or PTEN in such a way as to ensure that the steady-state level of γ is just below the threshold. When stimulated by a chemoattractant gradient, only the front of the cell would have PI3K concentrations above the threshold, and this ensure that only the front would respond. This would then explain the extreme polarizations seen in *Dictyostelium* cells.

3.2.2 Oscillators and positive feedback

Besides providing for strong amplification, one of the uses of positive feedback in engineering circuits is as a means of designing oscillators. Experimentally, this was discovered around the 1915 when several inventors discovered the use of positive feedback to generate oscillatory signals [4].

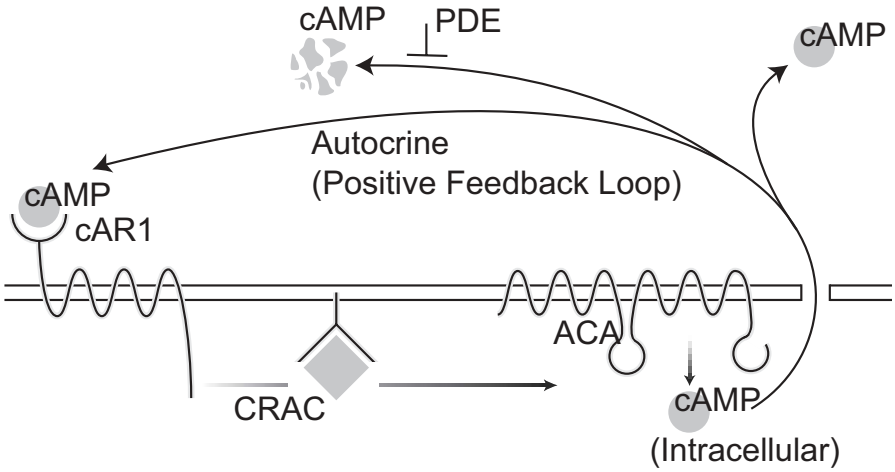

Fig. 24: **Autocrine loop.** One of the second messengers turned on by extracellular cAMP binding and resultant CRAC activation is the activation of the adenylyl cyclase of aggregation (ACA). This is a membrane bound protein that, when active, synthesizes cAMP. This intracellular cAMP is then secreted. The secreted cAMP can diffuse and signal other nearby cells; it can be destroyed by the phosphodiesterase PDE; or it may cycle back to signal the cell that synthesized it. This positive feedback loop is known as an autocrine loop.

One feature of the chemotactic signaling pathway of *Dictyostelium* is the autocrine loop shown in Fig. 24 involving cAMP. Autocrine loops arise when a cell secretes a chemical that stimulates the secretory cell itself.

Receptor binding of extracellular cAMP in *Dictyostelium* induces the activation of ACA which leads to the synthesis of intracellular cAMP from adenosine triphosphate (ATP). This cAMP is secreted into the extracellular medium where: 1) it can diffuse away from the cell; 2) find its way back to the cell surface receptors; or, 3) be destroyed by the phosphodiesterase (PDE). A thorough analysis of autocrine loops is complicated by the stochastic nature of the motion that governs the return of the secreted molecule to the cell surface receptor [62], however, it is clear that a positive feedback loop is established. This positive feedback path is coupled to the negative feedback mechanism that provides adaptation described above. Together, these counteracting effects lead to the formation of cAMP waves that can propagate as circular or spiral wave forms.

In the model of [45], a negative feedback attributed to cAMP-induced receptor desensitization

through phosphorylation is introduced. We replace this desensitization with the adaptation mechanism outlined in Section 3. For the positive feedback model, we mirror closely the assumptions of [45], though the dynamics are simpler.

In particular, we first assume that the amount of concentration of internal cAMP is governed by the differential equation

$$\frac{dC(t)}{dt} = -\underbrace{k_1 C(t)}_{\text{degradation}} - \underbrace{k_2 C(t)}_{\text{secretion}} + \underbrace{k_3 [R^\star(t)]^2 + k_4}_{\text{synthesis}}$$

Here we have assumed that the amplification that is observed in the response of the cell is given by the quadratic dependence on $R^\star$ in the synthesis term. Also, we have added a small constant production term ($k_4 \ll 1$).

The external cAMP concentration is, in turn,

$$\frac{dS(t)}{dt} = -\underbrace{k_5 S(t)}_{\text{loss}} + \underbrace{k_6 C(t)}_{\text{secretion}}$$

Note that, though they involve the same material, the secretion terms differ because of the differences in volume between the internal and extracellular media. Also, the loss term in extracellular cAMP includes that lost/gained from neighbouring cells as well as that degraded by the phosphodiesterase.

These equations are now coupled to (16), (18) and (19). To simplify the analysis, we will assume that the equations governing $R^\star$, A and C are all "fast" so that we may replace these variables in the remaining two differential equations by their steady-state values. In particular, we see that the system reduces to

$$\begin{aligned}
\frac{dI(t)}{dt} &= -a_1 I(t) + a_2 S(t) \\
\frac{dS(t)}{dt} &= -a_3 I(t) + \frac{a_4 S^2(t)}{(a_5 S(t) + I(t))^2} + a_6
\end{aligned}$$

where $a_1 = k_{-i}$, $a_2 = k_i$, $a_3 = k_5$, $a_4 = k_3 k_6 k_a^2 k_r^2 R_T^2 / [(k_1 + k_2)(k_{-a}^2 k_{-r}^2)]$, $a_5 = k_r k_a / (k_{-r} k_{-a})$, and $a_6 = k_4 k_6 / (k_1 + k_2)$. The system can be simplified further by defining states

$$x = \frac{a_2^2 a_3}{a_1^2 a_4} S, \quad y = \frac{a_2 a_3}{a_1 a_4} I$$

a new "time" $\tau = a_3 t$, yielding

$$\dot{x} = -x + \frac{x^2}{(ax+y)^2} + \varepsilon =: f(x,y) \tag{23}$$

$$\dot{y} = -b(y - x) =: g(x,y) \tag{24}$$

with $a = a_1 a_5 / a_2$, $b = a_1 / a_3$ and $\varepsilon = a_2^2 a_6 / (a_1^2 a^4)$. A phase-plane analysis for this system is given in Fig. 25. The equilibrium $x = y \approx 1/(1+a)^2$ is stable iff $b > (1-a)/(1+a)$. Using the Poincaré-Bendixson theorem, it is straightforward to show that a stable limit cycle exists when this condition fails.

This simple model can account for the autonomous oscillations observed experimentally. Other models can also account for the synchronization seen in cells [42, 49]. While these models differ into the biochemical identities of activators and inactivators they all rely on an interplay between positive and negative feedback to achieve this periodic oscillation.

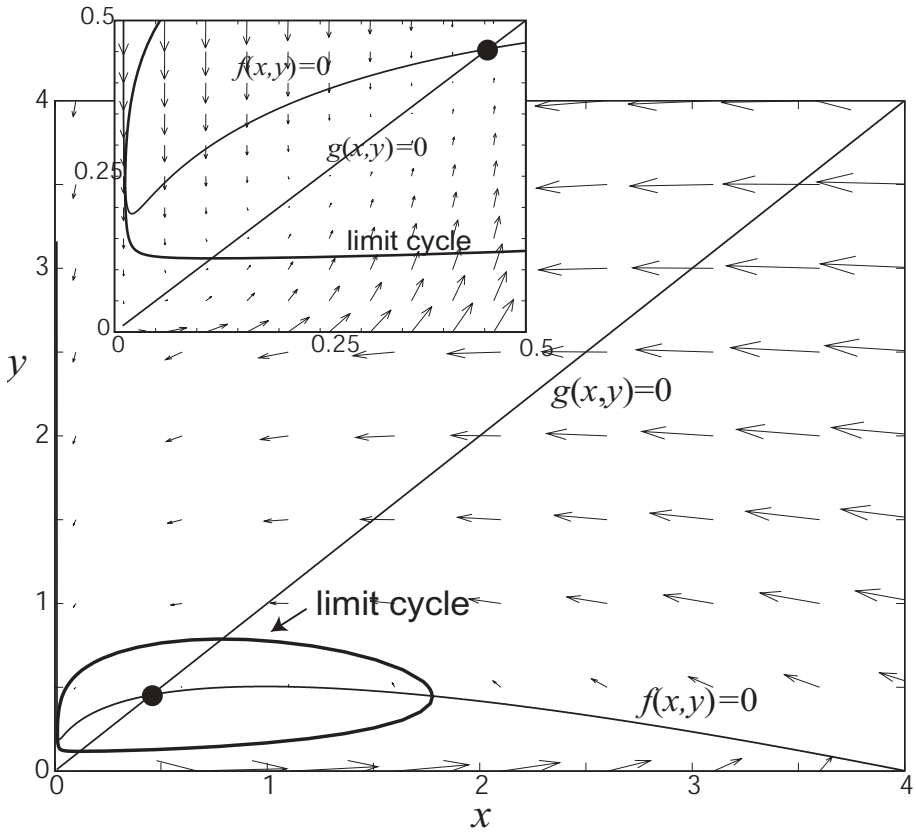

Fig. 25: **Limit cycle oscillation.** Shown is the phase-plane analysis for the oscillator of (23) and (24). Specifically, the parameters $a = 1/2$, $b = 1/6$ and $\varepsilon = 0.01$ were chosen so as to make the equilibrium point at $x = y = 4/9$ unstable. Note that the nullcline for $g(x,y)$ increases sharply as $x \downarrow \varepsilon > 0$ (see the insert). This allows application of the Poincaré-Bendixson theorem.

3.2.3 Memory and positive feedback

One final use of positive feedback in engineering systems is through the creation of a bistable system. This principle is the basis on which such electrical components as the Schmitt trigger are designed [59]. Schmitt triggers combine high gain amplifiers with positive feedback to obtain transfer functions with hysteresis. The resulting circuit is bistable — that is, it has two stable equilibria. The bistable system demonstrates bistability as the response of the circuit at any moment is not determined solely by the value of the input signal at that moment in time, but insteady by both the value of the input *and* the state of the system.

Bistable systems in biology have been studied extensibly by Ferrell [19]. In *Dictyostelium* chemotaxis, the use of bistability has not been demonstrated conclusively. However, it is known that highly polarized cells do exhibit a hysteretic memory while chemotaxing [13]. Moreover, this memory requires an active cytoskeleton, as cells that have been immobilized by the addition of Latrunculin A do not show this memory. It is therefore likely that positive feedback through the cytoskeleton could provide this memory.

3.3 Discussion

In recent years, biology has undergone a revolution. Traditionally, biologists have taken studied signaling pathways by "breaking" these networks into their components to study them separately. While this reductionist paradigm has led to many breakthroughs, it alone cannot provide a full understanding of the system.

High-throughput technologies characteristic of the "genomic" and "proteomic" fields have emerged which provided biologists with detailed parts lists of the systems involved.

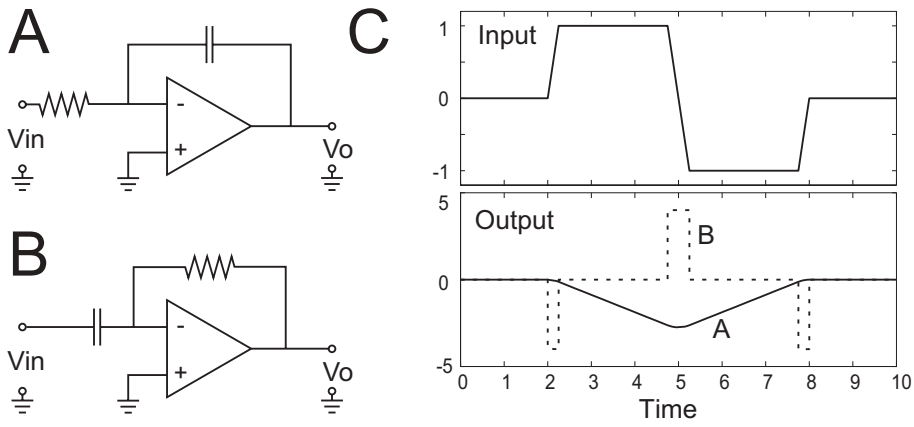

Fig. 26: **Same parts, different outputs.** The circuits on the left demonstrate why knowing the parts list of a circuit is not enought to know its function. A. The amplifier, resistor and capacitor are configured with the capacitor in the feedback loop. B. The same three circuit elements are reconnected in B with the resistor in the feedback path. C. The response of the systems. That from panel A (solid line) acts as an integrator of the input voltage V_{in} whereas that from B (dashed line) acts in the completely opposite way, as a differentiator.

Clearly, having a complete list of parts is desirable, but not sufficient to elucidate function. The engineering example illustrated in Fig. 26 points to some of the possible problems. Here, three electrical components: a resistor, operational amplifier and a capacitor, are arranged in two separate configurations. A voltage input V_{in} is applied to both systems and the output voltage V_{o} is then measured. As illustrated in Fig. 26C, the system in Fig. 26A (solid line) acts as an integrator ($V_{\text{o}} = \int_0^t V_{\text{in}}(\tau)\text{d}\tau$) whereas that in Fig. 26B (dotted line) is a differentiator (i.e. $V_{\text{o}} = dV_{\text{in}}(t)/dt$.) Thus while the components of the two systems are the same, their behaviors are complete opposites.

In biology, much time and effort has been spent in discovering the components. As this example shows, however, it is not only the "parts list" of the system that determines the behavior of the system, but how these components are connected. To understand the function of these systems it will be necessary to have an understanding of how complex systems perform. A new field: "systems biology" has emerged, in which the behaviour and relationships of all of the elements in a particular biological system are investigated simulataneously while it is functioning [27, 38, 39]. Concepts from engineering play a crucial role in this new field, including modularity, robustness, amplification, adaptation, etc. [22].

In this paper I have tried to illustrate the similarities between traditional control engineering tasks such as robust disturbance rejection and amplification and those of signaling transduction pathways. It should be clear that a control engineering understanding of these systems will greatly facilitate the "reverse engineering" of these systems leading to a thorough understanding of their function.

Acknowledgements

The work of PAI was supported in part by the Whitaker Foundation and the National Science Foundation's Biocomplexity program, through grant number DMS-0083500.

References

[1] Acerenza L, Sauro HM, Kacser H. Control analysis of time-dependent metabolic systems. J Theor Biol. 1989 Apr 20;137(4):423–44.

[2] Alon U, Surette MG, Barkai N, Leibler S. Robustness in bacterial chemotaxis. Nature 1999; 397: 168–171.

[3] Barkai N, Leibler S. Robustness in simple biochemical networks. Nature. 1997 Jun 26;387:913–7.

[4] Bennett S. A history of control engineering: 1800–1930. Peter Peregrinus, Stevenage, UK 1979.

[5] Berg HC, Brown DA. Chemotaxis in *Escherichia coli* analysed by three-dimensional tracking. Nature. 1972 Oct 27; 239:500–4.

[6] Bode HW Network Analysis and Feedback Amplifier Design, Van Nostrand, New York, 1945.

[7] Bray D, Bourret RB, Simon MI. Computer simulation of the phosphorylation cascade controlling bacterial chemotaxis. Mol Biol Cell. 1993 May;4(5):469–82.

[8] Brugge JS, McCormick F. Cell regulation: Intracellular networking. Curr Opin Cell Biol 1999; 11: 173–176.

[9] Chung CY, Funamoto S, Firtel RA. Signaling pathways controlling cell polarity and chemotaxis. Trends Biochem Sci 2001; 26: 557–566.

[10] Cockroft S. Biology of phosphoinositides. Oxford University Press, Oxford 2000.

[11] Czech MP. PIP2 and PIP3: complex roles at the cell surface. Cell 1999; 100: 603–606.

[12] Demin OV, Westerhoff HV, Kholodenko BN. Control analysis of stationary fixed oscillations. J. Phys. Chem. B 1999; 103: 10695–710.

[13] Devreotes P, Janetopoulos C. Eukaryotic chemotaxis: distinctions between directional sensing and polarization. J Biol Chem. 2003 Jun 6;278(23):20445–8.

[14] Doedel EJ. Cong Numer 1981; 30:265–384.

[15] Doyle JC, Francis BA, Tannenbaum AR. Feedback Control Theory. Macmillan, New York, 1992.

[16] Doyle, J., personal communication.

[17] El-Samad H, Goff JP, Khammash M. Calcium homeostasis and parturient hypocalcemia: an integral feedback perspective. J Theor Biol. 2002 Jan 7;214(1):17–29.

[18] Fell DA. Metabolic control analysis: a survey of its theoretical and experimental development. Biochem J. 1992 Sep 1;286 (Pt 2):313–30.

[19] Bagowski CP, Ferrell JE Jr. Bistability in the JNK cascade. Curr Biol. 2001 Aug 7;11(15):1176–82.

[20] Francis BA, Wonham WM. Automatica 1975; 12:457–465.

[21] Goodwin B. Oscillatory behavior in enzymatic control processes. Advances in Enzyme Regulation 1965; 3:425–438.

[22] Hartwell LH, Hopfield JJ, Leibler S, Murray AW. From molecular to modular cell biology. Nature. 1999 Dec 2; 402:C47-52.

[23] Hauri DC, Ross J. A model of excitation and adaptation in bacterial chemotaxis. Biophys J. 1995 Feb;68(2):708–22

[24] Heinrich R, Reder C. Metabolic control analysis of relaxation processes. J Theor Biol 1991; 151:343–350.

[25] Heinrich R, Schuster S. The Regulation of Cellular Systems, Chapman & Hall, New York, 1996.

[26] Hofmeyr, J-HS. Metabolic control analysis in a nutshell, Proceedings of the International Conference on Systems Biology, Pasadena, California, pp. 291–300, 2000.

[27] Ideker T, Galitski T, Hood L. A new approach to decoding life: systems biology. Annu Rev Genomics Hum Genet 2001; 2:343–372.

[28] Iglesias PA, Levchenko A. A general framework for achieving integral control in chemotactic biological signaling mechanisms. Proc 40th IEEE Conference on Decision and Control, Orlando, FL, pp. 843–848, 2001.

[29] Iglesias PA, Levchenko A. Spatial sensing in *Dictyostelium*: Amplification through saturating nonlinearities. In: First Intern Conf Systems Biology, Tokyo, Japan, pp 154–159, 2000.

[30] Iglesias PA, Levchenko A. Modeling the cell's guidance system. Sci STKE 2002; 2002: RE12.

[31] Iijima M, Devreotes P. Tumor suppressor PTEN mediates sensing of chemoattractant gradients. Cell 2002; 109: 599–610.

[32] Iijima M, Huang YE, Devreotes P. Temporal and spatial regulation of chemotaxis. Dev Cell 2002; 3: 469–478.

[33] Ingalls BP, Sauro HM. Sensitivity analysis of stoichiometric networks: an extension of Metabolic Control Analysis to non-equilibrium trajectories. J. Theor. Biol. 2003; 222:23–36.

[34] Isidori A, Byrnes CI. IEEE Trans. Auto. Control 1990; 35:131–140.

[35] Kascer H, Burns JA. The control of flux, Symp. Soc. Exp Biol 1973; 27:65–104.

[36] Kessin RH. *Dictyostelium*: evolution, cell biology, and the development of multicellularity. Cambridge UP, Cambridge 2001.

[37] Kholodenko BN, Demin OV, Westerhoff HV. Control analysis of periodic phenomena in biological systems. J Phys Chem B 1997; 101:2070–2081.

[38] Kitano H. Systems biology: a brief overview. Science 2002; 295: 1662–1664

[39] Kitano H. Computational systems biology. Nature 2002; 420: 206–210.

[40] Kohn MC, Whitley LM, Garfinkel D. Instantaneous flux control analysis for biochemical systems. J Theor Biol 1979; 76:437–452.

[41] Krishnan J, Iglesias PA. Analysis of an adaptation module of gradient sensing. Bulletin of Mathematical Biology 2003; 67: 95–128.

[42] Laub MT, Loomis WF. A molecular network that produces spontaneous oscillations in excitable cells of *Dictyostelium*. Mol Biol Cell 1998; 9: 3521–3532.

[43] Levchenko A, Iglesias PA. Models of eukaryotic gradient sensing: application to chemotaxis of amoebae and neutrophils. Biophys. J. 2002; 82: 50–63.

[44] Lynn PA. An Introduction to the Analysis and Processing of Signals, 2nd edition, MacMillan Press, London, 1982.

[45] Martiel J-L, Goldbeter A. A model based on receptor desensitization for cyclic AMP signaling in *Dictyostelium* cells. Biophys. J. 1987; 52: 807–828.

[46] Meinhardt H. Orientation of chemotactic cells and growth cones: models and mechanis ms. J. Cell Sci. 1999; 112: 2867–2874.

[47] Ming GL, Wong ST, Henley J, Yuan XB, Song HJ, Spitzer NC, Poo MM. Adaptation in the chemotactic guidance of nerve growth cones. Nature. 2002 May 23;417(6887):411-8.

[48] Morris, K. Introduction to Feedback Control, Harcourt Academic Press, London, 2001.

[49] Nagano S. Diffusion-assisted aggregation and synchronization in *Dictyostelium discoideum*. Phys Rev Lett 1998; 80: 4826–4829.

[50] Narang A., Subramanian KK, Lauffenburger DA. A mathematical model for chemoattractant gradient sensing based on receptor-regulated membrane phospholipid signaling dynamics. Ann Biomed Eng 2001; 29: 677–691.

[51] Parent CA, Devreotes PN. A cell's sense of direction. Science 1999; 284: 765–770.

[52] Postma M, Van Haastert PJ. A diffusion-translocation model for gradient sensing by chemotactic cells. Biophys J 2001; 81: 1314–1323.

[53] Rappel WJ, Thomas PJ, Levine H, Loomis WF. Establishing direction during chemotaxis in eukaryotic cells. Biophys. J. 2002; 83: 1361–1367.

[54] Reder C. Metabolic control theory: a structural approach, J Theor Biol 1988; 135:175–201.

[55] Reijenga KA, Westerhoff HV, Kholodenko BN, Snoep JL. Control analysis for autonomously oscillating biochemical networks. Biophys J. 2002 Jan;82(1 Pt 1):99-108.

[56] Samoilov M, Arkin A, Ross J. Signal processing by simple chemical systems. J. Phys. Chem. A 2002; 106:10205–10221.

[57] Santillán M, Mackey, MC. Dynamic regulation of the tryptophan operon: A modeling study and comparison with experimental data. Proc. Natl. Acad. Sci. USA 2001; 98:1364–1369.

[58] Savageau MA. Biochemical Systems Analysis. A Study of Function and Design in Molecular Biology, Addison-Wesley, Reading, MA, 1976.

[59] Sedra AS, Smith KC. Microelectronic circuits. Holt, Rinehart and Winston, New York, 1982.

[60] Segall JE, Manson MD, Berg HC. Signal processing times in bacterial chemotaxis. Nature. 1982 Apr 29; 296:855-7.

[61] Segel LA, Goldbeter A, Devreotes PN, Knox BE. A mechanism for exact sensory adaptation based on receptor modification. J Theor Biol. 1986 May 21;120(2):151-79.

[62] Shvartsman SY, Wiley HS, Deen WM, Lauffenburger DA. Spatial range of autocrine signaling: modeling and computational analysis. Biophys J 2001; 81: 1854–1867.

[63] Spiro PA, Parkinson JS, Othmer HG. A model of excitation and adaptation in bacterial chemotaxis. Proc Natl Acad Sci U S A. 1997 Jul 8;94(14):7263-8.

[64] Stock JB, Lukat GS, Stock AM. Bacterial chemotaxis and the molecular logic of intracellular signal transduction networks Annu Rev Biophys Biophys Chem. 1991; 20:109-36.

[65] Strang G. Introduction to Applied Mathematics, Wellesley-Cambridge Press, Wellseley, MA, 1986.

[66] Strogatz SH. Nonlinear Dynamics and Chaos. Addison-Wesley Publishing Company, Reading, MA, 1994.

[67] Voit EO. Computational Analysis of Biochemical Systems. Cambridge University Press, Cambridge, 2000.

[68] Weiner OD, Neilsen PO, Prestwich GD, Kirschner MW, Cantley LC, Bourne HR. A PtdInsP(3)- and Rho GTPase-mediated positive feedback loop regulates neutrophil polarity (2002) Nat Cell Biol 4: 509–513.

[69] Xiu ZL, Zeng AP, Deckwer WD. Multiplicity and stability analysis of microorganisms in continuous culture: effects of metabolic overflow and growth inhibition. Biotechnol Bioeng. 1998 Feb 5;57(3):251-61.

[70] Yi TM, Huang Y, Simon MI, Doyle J. Robust perfect adaptation in bacterial chemotaxis through integral feedback control. Proc Natl Acad Sci U S A. 2000 Apr 25;97(9):4649–53.